M 2023

U.PORTO
FEUP FACULDADE DE ENGENHARIA
UNIVERSIDADE DO PORTO

ENERGY AND ECONOMIC ANALYSIS OF A HYDROGEN PURIFICATION SYSTEM FROM WATER ELECTROLYSIS

INÊS NUNES RODRIGUES

MASTER THESIS IN CHEMICAL ENGINEERING
PRESENTED TO THE FACULTY OF ENGINEERING
OF THE UNIVERSITY OF PORTO

Master in Chemical Engineering

Energy and economic analysis of a hydrogen purification system from water electrolysis

Master dissertation

of

Inês Nunes Rodrigues

Developed within the course of dissertation

held in

Amnis Pura, Ltd

Supervisor at FEUP: **Dr. Paulo Ribeirinha**

Joint supervisor at FEUP: **Prof. Adélio Mendes**

Coordinator at Amnis Pura: **Dr. Frederico Relvas**

March 2023

Acknowledgment

Firstly, I would like to thank my supervisor, Dr. Frederico Relvas, for all the orientation and support throughout the development of this dissertation. I would also like to thank my two supervisors in FEUP, Dr. Paulo Ribeirinha and Prof. Adélio Mendes, for giving me the opportunity to learn and work in such an interesting area.

A special thanks to Tiago Santos, for always being available to help. And to everyone in Amnis Pura, in particular, Carlos and José Pedro, thanks for the concern, and showing me how things worked in practice.

To my amazing friends, who were by my side in this journey in FEUP and with who I made unforgettable memories. A special thanks to Sara, for being my family in Porto. Also thank you Maria for always being there for me and Miguel for all the help in and out of the university. Also, thanks Emanuel for the constant guidance while also showing me the academic life. To Diogo, thank you for all your patience, support and giving me strength to keep fighting.

And last but not least, thanks to my family, for the unconditional support in good and bad moments. To my brother, for giving me encouragement and to my grandparents, whose kind and wise words always improve my day. And most importantly, to my parents, who I could never thank enough for providing me everything they could. To my mother, from who I inherited the curiosity, open-mindedness and interest for science that led me here today, thank you for motivating me and always trying to help even when I think I don't need it. And thank you to my father, whose kindness and resilience always brought me comfort in hard times and made me not give up, and for making me want to leave the world a little better than I found it.

A todos, o meu bem-haja.

Abstract

In order to achieve net zero CO_2 emissions, the development of green technologies such as electrolysers and fuel cells is necessary. Hydrogen can be obtained through water electrolysis and further used in fuel cells to generate energy. However, the hydrogen that exits the electrolyser is saturated with water and requires purification in order to be utilized in the fuel cells. Therefore, a drying step after electrolysis is required, which is typically achieved by Pressure Swing Adsorption (PSA), an established gas separation technology. Two variants of this method, Vacuum Pressure Swing Adsorption (VPSA) and Temperature Swing Adsorption (TSA) may also be used for the same purpose.

In this work, the hydrogen purification system was assessed in order to determine which technology is the most suitable for meeting the fuel cell requirements, which correspond to a water content of less than 5 ppm. Preliminary studies revealed that when recycling is implemented, energy and product waste are significantly reduced.

Additionally, when evaluating the three technologies, it was shown that for a lower operating pressure of 20 bar, the required purity is achieved with lower energy consumption, due to less compression work. The VPSA system presented an advantage in comparison to the others in terms of energy required per mass of purified hydrogen. When operating with a feed flowrate of 30 $Nm^3 \cdot h^{-1}$ at this pressure, a consumption of 0.45 $kWh \cdot kg^{-1}$ was achieved.

The economic analysis revealed that the feed flow rate has a significant contribution on the profitability of the system, as the fixed costs are relatively cut down for higher product flows. Moreover, the TSA system required the smallest investment in terms of equipment and the lowest operating costs. Based on the economic measure Levelized Cost of Energy (LCOE), TSA was the most economically advantageous process. For 20000 $Nm^3 \cdot h^{-1}$ and an operating pressure of 20 bar, it was obtained a LCOE of 0.14 $€ \cdot kWh^{-1}$.

In conclusion, although VPSA consumes less energy per amount of product, TSA requires less capital investment and overall is considered the most efficient process for hydrogen purification from electrolysis, when both energy and economic aspects are considered.

Keywords: **PSA, VPSA, TSA, Hydrogen, Purification**

Resumo

De modo a atingir zero emissões líquidas de CO_2, o desenvolvimento de tecnologias verdes como eletrolisadores e células de combustível é necessário. O hidrogénio pode ser obtido através de eletrólise da água e posteriormente usado em células de combustível para gerar energia. No entanto, o hidrogénio que sai do eletrolisador está saturado com água e requer purificação de modo a ser utilizado nas células de combustível. Assim, um passo de secagem depois da eletrólise é indispensável, o que é normalmente conseguido por Pressure Swing Adsorption (PSA), uma tecnologia estabelecida de separação de gases. Duas variantes deste método, Vacuum Pressure Swing Adsorption (VPSA) e Temperature Swing Adsorption (TSA) também podem ser usadas para o mesmo propósito.

Neste trabalho, o sistema de purificação de hidrogénio foi avaliado de modo a determinar que tecnologia é a mais adequada para atingir os requisitos das células de combustível, que correspondem a um teor de água inferior a 5 ppm. Estudos preliminares revelaram que quando reciclo é implementado, o desperdício de energia e produto são significativamente reduzidos.

Adicionalmente, quando as três tecnologias foram avaliadas, mostrou-se que para uma pressão de operação de 20 bar, a pureza requerida é atingida com o menor consumo energético, devido a menos trabalho de compressão. O sistema de VPSA apresentou uma vantagem em comparação aos outros em termos de energia necessária por massa de hidrogénio purificado. Operando com um caudal de alimentação de 30 $Nm^3 \cdot h^{-1}$ e a esta pressão, um consumo de 0.45 $kWh \cdot kg^{-1}$ foi atingido.

A análise económica revelou que o caudal de alimentação tem uma contribuição significativa na lucratividade do sistema, uma vez que os custos fixos são relativamente abatidos para caudais de produto superiores. Além disso, o sistema de TSA requer o menor investimento em termos de equipamento e os menores de operação. Baseado na medida económica do custo normalizado da energia (LCOE), o TSA foi o processo economicamente mais vantajoso. Para 20000 $Nm^3 \cdot h^{-1}$ e pressão de operação de 20 bar, foi obtido um LCOE de 0.14 $€ \cdot kWh^{-1}$.

Concluindo, apesar do VPSA consumir menos energia por quantidade de produto, o TSA requer menor investimento capital e no geral é considerado o processo mais eficiente para purificação de hidrogénio proveniente da eletrólise, quando ambos os aspetos energético e económico são considerados.

Palvavras-Chave: **PSA, VPSA, TSA, Hidrogénio, Purificação**

Declaration

I hereby declare, under word of honour, that this work is original and that all non-original contributions is indicated and due reference is given to the author and source

Porto, 13 March 2023

(Inês Nunes Rodrigues)

Index

List of Figures

List of Tables

Notation and Glossary

A	area	m^2
C_B	base cost	€
C_p	specific heat capacity	$kJ \cdot kg^{-1} \cdot K^{-1}$
C_P	purchase cost	€
d_p	pore diameter	nm
E	energy expenditures	€
F	electricity generation	kWh
F_D	drive factor	
F_M	material factor	
F_P	pressure factor	
H	hydrogen generation	kg
I	investment expenditures	€
L/D	length to diameter ratio	
M	maintenance expenditures	€
P	pressure	Pa
P_c	consumed power of compressor	hp
r	discount rate	
S_g	surface area	$m^2 \cdot g^{-1}$
t	year of operation	y
V_p	pore distribution	$cm^3 \cdot g^{-1}$

Greek Letters

ϵ	porosity	
ρ	mass density	$kg \cdot m^{-3}$

Indexes

0	year 0
t	year t

List of Acronyms

AEM	Anion-Exchange Membrane
AWE	Alkaline Water Electrolysis
CAPEX	Capital Expenditures
CCUS	Carbon Capture, Utilisation and Storage
CEPCI	Chemical Engineering Plant Cost Index
FCI	Fixed-Capital Investment
LCOE	Levelized Cost of Electricity
LCOH	Levelized Cost of Hydrogen
OPEX	Operational Expenditures
PEM	Polymer Electrolyte Membrane
PSA	Pressure Swing Adsorption
ROI	Return On Investment
SOE	Solid Oxide Electrolysis
TCI	Total Capital Investment

TSA	Temperature Swing Adsorption
VPSA	Vacuum Pressure Swing Adsorption
WC	Working Capital

1 Introduction

1.1 Framing and presentation of the work

Global energy demand is increasing due to emerging markets and developing economies. Simultaneously, the rising concern about climate change requires a transition to cleaner energy technologies with fewer greenhouse gas emissions and sustainable production and consumption. In order to achieve net zero CO_2 emissions, the International Energy Agency presented key pillars to the decarbonisation of the global energy system, which include energy efficiency, electrification, renewable energy, hydrogen and hydrogen-based fuels (International Energy Agency, 2021).

Hydrogen is a light, storable gas that is considered a clean, flexible energy carrier. Currently, it is most commonly used in industry for oil refining and ammonia production. However, it can also be used as fuel in fuel cells and generate electricity and heat, with various potential uses in the transport and energy sectors. Therefore, hydrogen plays an important role in the global energy transition (Hydrogen Council, 2022). Nevertheless, to make a significant contribution, hydrogen sources and production processes have great impact. There are three main colours in which hydrogen can be categorized depending on its production process, as represented in Figure 1.1.

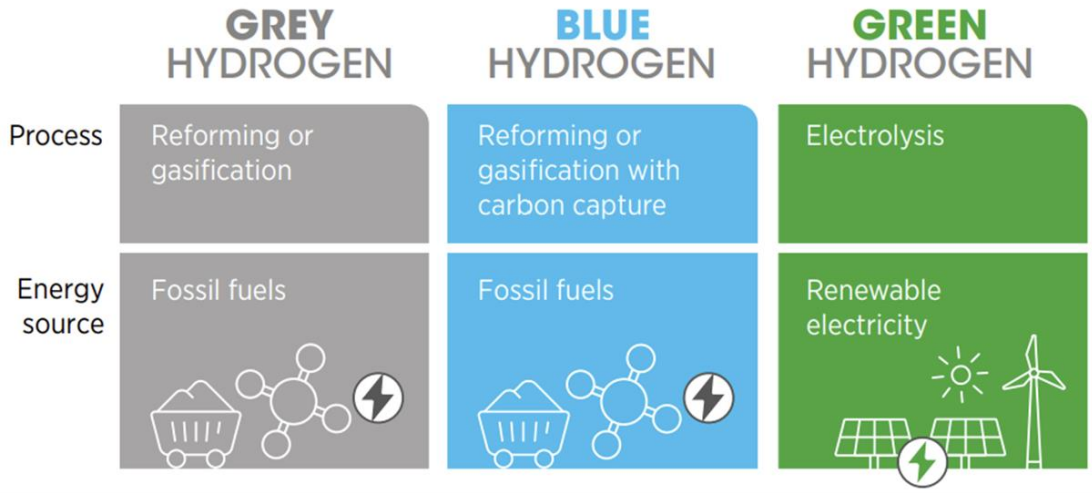

Figure 1.1 – Selected colour-code typology of hydrogen production. Extracted from International Renewable Energy Agency (2022).

Hydrogen production by splitting water into oxygen and hydrogen (water electrolysis) does not have CO_2 as by-product, hence not generating carbon emissions nor requiring its capture. By using renewable energy sources for the electricity required, “green hydrogen” is obtained and the process is considered carbon-neutral (International Renewable Energy Agency, 2022).

However, this process is still under study and one of its major drawbacks is the current high cost across its entire value chain. In 2021, the average cost of hydrogen production from natural gas without CCUS (carbon capture, utilisation and storage) was in the range of 1.0-2.5 $\$\cdot kg_{H2}^{-1}$ while via electrolysis with renewable electricity was at 4.0-9.0 $\$\cdot kg_{H2}^{-1}$ (International Energy Agency, 2022).

Moreover, the obtained hydrogen contains impurities and in order to be utilized in fuel cells, it requires certain quality standards and purity (Bacquart *et al.*, 2018). The main contaminants found in hydrogen from electrolysis are water, oxygen and nitrogen. Water is the most difficult to remove (Ligen *et al.*, 2020) and in fuel cells, impurities present in water not only can reduce the membranes conductivity, but also cause corrosion of metal parts (Du *et al.*, 2021). Although various purification processes have been developed, their integration with the electrolyser as well as the outlet gas composition are still a work in progress.

Pressure Swing Adsorption (PSA) is the most common process for hydrogen purification (or drying) and is implemented by cyclic pressure changing on a bed column, based on the difference in the adsorbent capacity for different gases (Ligen *et al.*, 2020).

In this context, the main purpose of this work is an energy and economic analysis of a drying system to obtain high purity hydrogen coming from electrolysis at the lowest energy cost. The purification system is composed by a gas-liquid separator, a catalytic reactor for deoxygenation, and a drying unit, where adsorption occurs (through pressure swing, vacuum pressure swing or temperature swing adsorption). The main tasks of this study include the analysis of the different purification/drying processes for hydrogen, simulation of the different processes involved and energy optimization and economic analysis for each case.

1.2 Presentation of the company

Amnis Pura is a spinoff company from the Faculty of Engineering of University of Porto and is one of the first companies dedicated to the development and commercialization of Pressure Swing Adsorption units for hydrogen purification. The company has, through its founders, more than 30 years of experience in purification processes.

1.3 Contribution of the author to the work

The processes studied can be mainly divided into two parts. The adsorption section was studied and evaluated based on existing works. The author was responsible for the development of this recycling section. Both the energy and economic analysis for the processes were performed by the author.

1.4 Organization of the dissertation

The present work is organized in six main chapters:

- In chapter one, **Introduction**, a framework for the dissertation subject is discussed as well as its main goals.
- In chapter two, **Context and State of the art**, a background on the most relevant technologies for hydrogen production and purification is presented, emphasizing on electrolysis to obtain green hydrogen and Pressure Swing Adsorption and its variants for its purification, a brief economic analysis is also presented.
- In chapter three, **Materials and Methods**, the methodology used to obtain the results is defined, the different scenarios under study are presented and a description of the systems under study is provided.
- In chapter four, **Results and Discussion**, the results obtained for the energy and economic analysis are presented and discussed as well as the different scenarios considered.
- In chapter five, **Conclusions**, the main conclusions of this work are presented as well as suggestions for future work.
- Finally, in chapter six, **Assessment of the work done**, a final review and evaluation of the work is provided and the defined objectives are analyzed.

2 Context and State of the art

2.1 Hydrogen

Hydrogen has a potential important role in the global energy transition. It is considered a clean fuel and on a mass basis, it displays an energy density of 120 $MJ \cdot kg^{-1}$, which is almost three times the energy content of gasoline (46 $MJ \cdot kg^{-1}$) (U.S. Department of Energy, n.d.) and five times of coal (24 $MJ \cdot kg^{-1}$). However, on a volume basis, liquid hydrogen has a density of 8 $MJ \cdot L^{-1}$, while gasoline has a density of 32 $MJ \cdot L^{-1}$ (University of Calgary, n.d.). As an energy carrier, hydrogen can store and deliver a great amount of energy and when used in fuel cells, it generates electricity and heat. In recent years, clean hydrogen has received increasing political and business attention, due to decreasing costs from renewable sources and increasing urgency on decarbonization and renewable energy demand (International Renewable Energy Agency, 2022). Ensuring a clean hydrogen supply is essential and already technically viable today. Nonetheless, further research is required in order to develop hydrogen economy and hydrogen as a fuel of the future (Veras *et al.*, 2017).

2.1.1 Hydrogen production

Despite being the most abundant gas in the universe, hydrogen is not found free in nature but it can be obtained from a variety of resources, including fossil fuels and renewable sources. Hydrogen production from fossil fuels is achieved by reforming technologies (steam reforming, partial oxidation and autothermal reforming), hydrocarbon pyrolysis or coal gasification. A renewable alternative is converting biomass to hydrogen through biological processes (dark fermentation and photofermentation) or thermochemical methods (pyrolysis, gasification and hydrothermal liquefaction). However, a carbon-neutral option exists: splitting water into hydrogen and oxygen using an electrical current (electrolysis). Other processes can be used for water-splitting, such as thermal energy (thermolysis) and photonic energy (photoelectrolysis) or through microorganisms (biophotolysis) (Megía *et al.*, 2021).

In 2021, hydrogen production reached 94 million tonnes (Mt), almost entirely obtained through fossil fuels, resulting in emissions of more than 900 Mt CO_2. Most hydrogen (62%) was produced via natural gas reforming without carbon capture, 19% obtained from coal and 18% as a by-product of naphtha reforming. Low-emission hydrogen represented less than 1 Mt (0.7%), almost all from fossil fuels with CCUS, with only 35 kt from water electrolysis. Although a very small amount was produced via electrolysis, this process saw an increase of almost 20% compared to 2020, reflecting an expanding implementation of such method (International Energy Agency, 2021).

2.1.1.1 Water electrolysis

Water electrolysis uses electricity to split water into hydrogen and oxygen, according to the reactions expressed in Equations 2.1-2.3 in Table 2.1. Because the water splitting is an nonspontaneous reaction, electricity is required. When this process is powered by a low carbon electricity source (such as wind, sea wave or biomass), it becomes a promising alternative for hydrogen production with zero CO_2 emissions (Megía *et al.*, 2021).

Table 2.1 – Half reactions and overall reaction of water electrolysis.

Anode	$H_2O \rightarrow ½\ O_2 + 2H^+ + 2e^-$	(2.1)
Cathode	$2H^+ + 2e^- \rightarrow H_2$	(2.2)
Overall	$H_2O \rightarrow H_2 + ½\ O_2$	(2.3)

As this reaction is endothermic, energy can be stored in the form of chemical bonds. The reverse reaction is exothermic and releases energy, making hydrogen a renewable energy source. Different technologies are available for water electrolysis (Jang *et al.*, 2022) according to the half-reactions, these include:

- Polymer electrolyte membrane (PEM) electrolysis: water is introduced in the anode, where it is split into protons (hydrogen ions H^+), which travel through a proton conductor membrane to the cathode to form H_2, while the oxygen remains with the water. Humidified polymer membranes act as the electrolyte and noble metals (platinum or iridium oxide) as electrocatalysts. Its operating temperatures range from 50 to 80 °C and pressure can be up to 30 bar. It is considered one of the most promising technologies for large scale due to lower investment cost and the higher lifetime (Dincer *et al.*, 2015). A PEM electrolyser is represented in Figure 2.1.
- Alkaline water electrolysis (AWE): water is introduced at the cathode, where the molecules dissociate and split into H_2 and hydroxide ions (OH^-), which travel to the anode in order to generate water and O_2. It uses KOH or NaOH aqueous solution as electrolyte and non-noble metal-based electrodes (nickel). It typically operates at 60–80 ◦C and a pressure of 30 bar.
- Solid oxide electrolysis (SOE): similar process to the alkaline water system, but it adds thermal energy. It uses a ceramic membrane of yttria-stabilized zirconia and operates in high-temperature conditions (600–1000 °C) (Jang *et al.*, 2022).
- Anion-exchange membrane (AEM) electrolysis: emerging technology that makes use of a semipermeable membrane to conduct anions while is impermeable to gases (Dawood *et al.*, 2020).

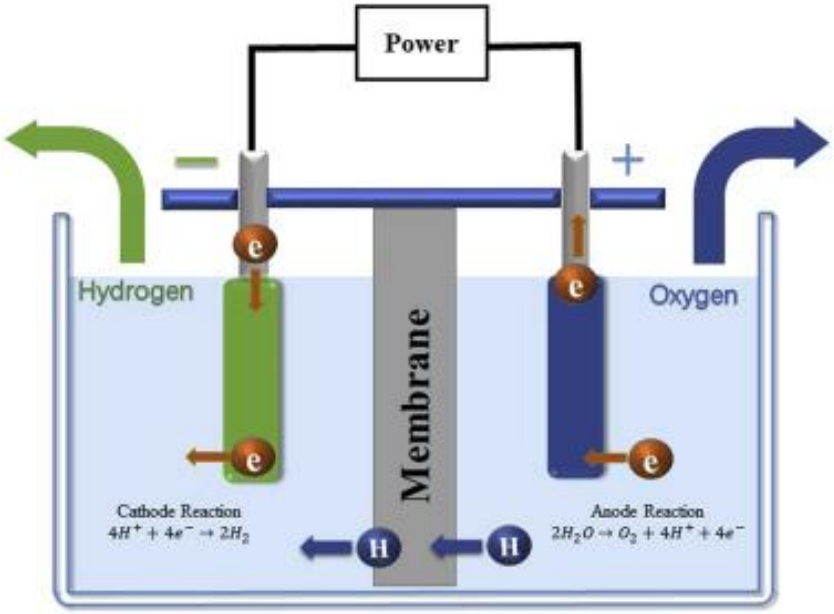

Figure 2.1 – Schematics of a PEM electrolyser. Extracted from Zhao (2021).

2.1.2 Transportation and storage

After being produced, hydrogen must be purified to meet the requirements for its end use. Purification technologies will be discussed in the following section (2.2) of this chapter. Due to hydrogen having a relatively low volumetric energy density, its transportation and storage can be challenging and are other important aspects of its value chain. The green hydrogen value chain is represented in Figure 2.2.

Hydrogen storage in large amounts can occur in three different forms: as a compressed gas at high pressures (over 200 bar), as a liquid at low temperatures (lower than -253 ºC) or dissolved in solids at lower pressures (less than 10 bar) (Associação Portuguesa para a Promoção do Hidrogénio. n.d.). For fuel cells power systems, hydrogen is stored as a compressed gas at 350 to 700 bar.

Large volumes of gaseous hydrogen can be transported through pipelines the same way as natural gas is today. In the absence of pipelines, hydrogen is liquefied and transported in insulated tanks. Although liquefaction consumes more than 30% of the energy content of the hydrogen, for longer distances it is more economical viable than trucking gaseous hydrogen, as it holds a much larger mass of hydrogen (U.S. Department of Energy, n.d.).

Capital investments, operating costs and energy requirements across the supply chain of hydrogen should be evaluated in order to respond to its growing demand. Green hydrogen offers various advantages, such as decarbonization, energy storage and easy distribution and for large scale applications. However, various factors significantly impact energy consumption,

equipment size and the recovery rate of this process, and consequently, production cost and overall efficiency. Because the purity of hydrogen depends on the adsorption pressure, for high concentration of impurities, large amounts of energy are necessary to pressurize the gas. For small scale units, this process becomes very energy intensive and less efficient, with the costs substantially increasing. Therefore, different options and parameters should be assessed in order to take advantage of this potentially green and efficient process (Nordio *et al*, 2021).

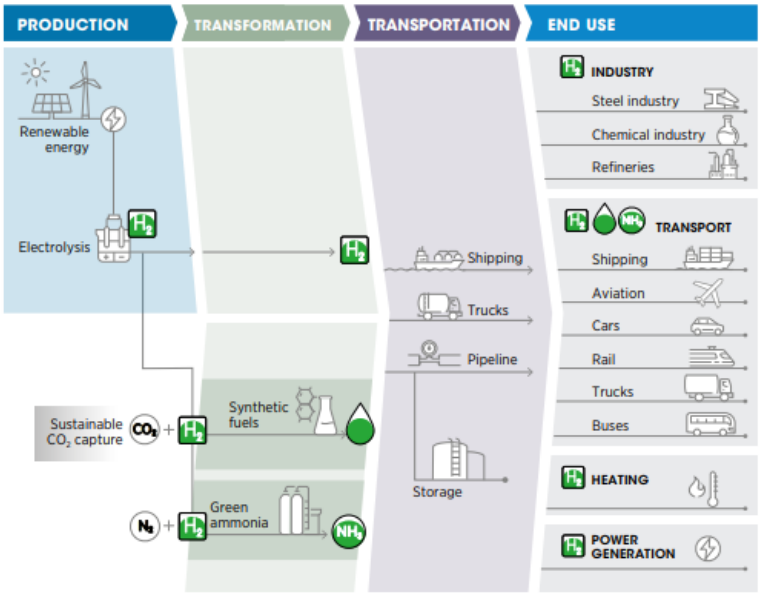

Figure 2.2 – Green hydrogen value chain. Extracted from International Renewable Energy Agency (2022).

2.2 Hydrogen purification

Purification is a crucial step to hydrogen's utilization, as the majority of its applications require high levels of purity. In order to be used as fuel, hydrogen quality is required to comply with the standards specified in ISO 14687:2019, which is in Annex A, including a minimum hydrogen fuel index of 99.97% (mole fraction) (International Organization for Standardization, 2019).

Depending on how it is produced, hydrogen may contain different impurities and for that reason, different purification methods can be applied. For electrolysis, out of the 13 components mentioned in ISO 14687:2019, only 3 of them are likely to be present in the hydrogen product. In Table 2.2, the typical content of these contaminants as well as the maximum content allowed is expressed, along with their probable origin and most common removal techniques (Ligen *et al.*, 2020).

Table 2.2 - Origin of hydrogen contaminants in alkaline electrolysis.

Contaminant	ISO threshold	Content without treatment	Origin	Treatment methods
Water	5 ppmv	>2000 ppm, saturated at ambient temperature	Process	Gas cooling, PSA or TSA systems
Oxygen	5 ppmv	2000-6000 ppm	Gas solubility, Cross over	Catalytic recombination $O_2 + 2H_2 \xrightarrow{-cat} 2H_2O$
Nitrogen	300 ppmv	<100 ppm after initial purge	Purge and inertization steps, Feed-in water	Venting of initial production

Nitrogen is used in the purge and inertization phases, in shut down or start up. Usually, no specific removal method is necessary and venting alone allows to reach the required levels. Oxygen can be considered a by-product of the hydrogen production through water electrolysis and is removed in a deoxygenation reactor. Water is the source for the hydrogen production and is also present in the product obtained. To be removed from the hydrogen stream, a few different purification methods can be used (Ligen *et al.*, 2020). Purification processes rely on physical or chemical principles and are usually based on adsorbing or condensing the impurities or using hydrogen-selective membranes. In some cases, electrochemical hydrogen compression may also be used (Vermaak *et al*, 2021). The most common purification processes and some of their characteristics are represented in Table 2.3.

Table 2.3 - Most common hydrogen purification processes. Retrieved from Dincer et al. (2015), Ruthven (1984) and Du et al. (2021).

	Method	Purity (%)	Temperature range (°C)	Pressure range (bar)	Advantages	Disadvantages
Adsorption	PSA	99.999	25-80	10-50 (outlet)	Ideal for large scale units, High-purity product, Long service life.	For higher purity levels lower recovery is achieved
	TSA		200-420	-	Good for strongly adsorbed species and desorbate can be highly recovered	High energy consumption, Large masses of adsorbent, Cycles limited by slow heating/cooling steps
	VPSA		25-80	Vacuum (10–2 mbar)	Lower energy consumption than PSA	Product delivered at sub-atmospheric pressure, Higher capital cost
Distillation	Cryogenic	99.8	(−235)–(−46)	1–10	Product easily stored as liquid, High hydrogen recovery	Highly energy-intensive, Not practical for high purity
Membranes	Porous	98	25-500	20	Ease of operation, Compact structure, Low investment cost and energy consumption, Cost effectiveness, Environmentally friendly	Not commercially viable
	Polymeric		25-65	Vacuum (10–2 mbar)		Highly permeable have lower selectivity
	Metallic (*e.g.* Pd)		350-500	>10		High manufacture costs, Prone to embrittlement
	Protonic		700-1000	>10		Not mature technology

2.2.1 Pressure Swing Adsorption Methods

Pressure Swing Adsorption (PSA) is by far the most widely used industrial process for hydrogen purification. The adsorption technology is based on gas molecules adhering to a solid adsorbent surface. PSA uses a bed of a solid adsorbent that, at a higher pressure, adsorbs impurities present in the inlet gas stream, and later desorbs them at a lower pressure, regenerating the adsorbent. The performance of this method varies according to the gas composition, the type of adsorbent and the partial pressure of the components.

PSA can be equilibrium- or diffusion-rate-based. Equilibrium-based separations are the most common, and rely on the ability of the adsorbent to adsorb more of "heavy" species than of "light" species at equilibrium, e.g., hydrogen is not as adsorbable as water vapor (Kohl *et al.*, 1997).

The basic two-bed pressure swing adsorption system is described by the Skarstrom cycle, which consists of four steps, described as follows and depicted in Figure 2.3:

1. Pressurization – feed gas enters the column, increasing its pressure up to the higher operating pressure;

2. Adsorption at high pressure - the heavy component (water vapor) is adsorbed while the light component (high purity dry hydrogen) is collected from the top of the column;

3. Depressurization - feed stops and part of the adsorbed impurities are removed as the heavy component exits through the bottom, depressurizing the unit, while hydrogen removed in this step is used to purge and pressurize another unit;

4. Purge at low pressure – light component flows in counter-current to purge the bed at low pressure, decreasing the partial pressure of the heavy component, causing it to desorb (Ruthven *et al.*, 1994).

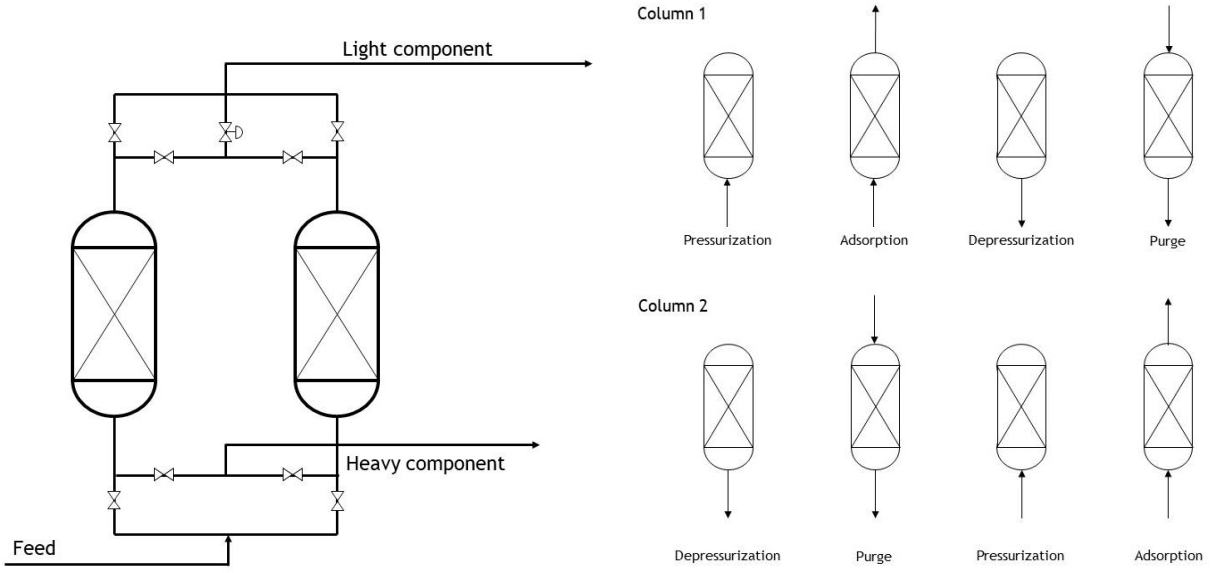

(a) (b)

Figure 2.3 – Schematic diagram (a) and sequence of steps (b) in a basic Skarstrom PSA cycle.

In the case of hydrogen purification, Skarstrom proposed a method for pressurizing a bed in a hydrogen purification PSA, the backfill step. This step involves feeding the column counter-currently using part of the purified gas. As a result, higher product purity and better recovery can be obtained. Furthermore, the backfill step allows the next column to be pressurized before the current one is emptied, ensuring that the product pressure and flow are continuous (Skarstrom, 1963). The proposed cycle is summarized in Figure 2.4.

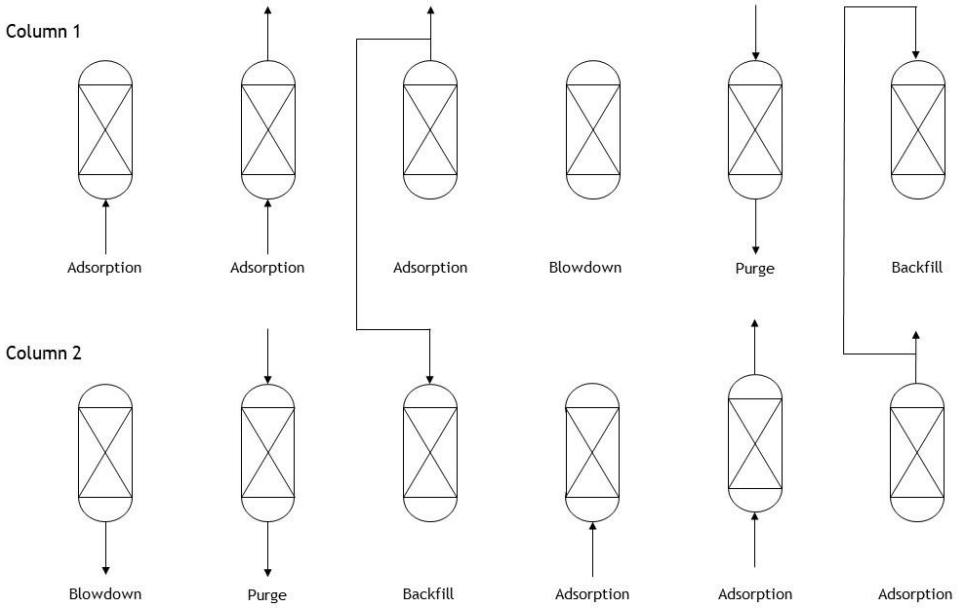

Figure 2.4 – Sequence of steps for a Skarstrom PSA cycle with backfill.

For PSA systems, feed pressure ideally ranges from 13 to 30 bar and a minimum pressure ratio of 4:1 between the adsorption and desorption steps is required for hydrogen purification (Kohl *et al.*, 1997).

As impurities are selectively concentrated on the surface of the adsorbent while the feed gas passes through, the selection of the adsorbent is of great importance to improve the efficiency of impurities removal. A broad variety of adsorbents has been studied but the most significant properties for its selection are selectivity, adsorption capacity, durability and cost. Additionally, it should be noted the specific surface area and pore size and distribution (Pourhakkak *et al.*, 2021).

In order to assess the adsorbent performance, most studies obtained equilibrium and kinetic data on fresh or "as received" adsorbents. Although a regeneration step is included in a PSA cycle, some irreversible adsorption may occur. In cyclic adsorption processes, the adsorbent contamination results in a progressive loss of adsorption capacity. Because after some cycles a "stationary state" is reached, an effective adsorption isotherm can be obtained. Ferreira *et al.* (Ferreira *et al.*, 2011) reported water vapor adsorption equilibrium isotherms on various adsorbents and concluded zeolites display better water vapor removal ability at lower relative pressures and may be the most appropriate for residual water vapor removal (ppm levels). On the other hand, for higher pressures, this ability increases significantly in activated alumina and silica gel. Due to their large adsorption capacity and easy regeneration, these are the most commonly used adsorbents in water vapor removal (Pourhakkak *et al.*, 2021). Additionally, the study found that the effective breakthrough time on a bed packed with silica is highly affected

by water vapor, unlike alumina (Ferreira *et al.*, 2011). Typical physical properties of the most used adsorbents in water adsorption for hydrogen purification are presented in Table 2.4. In this work, PSA and VPSA were considered using activated alumina and zeolite 4A was used for TSA.

Table 2.4 - Physical properties of the most used adsorbents for hydrogen purification. Retrieved from Pourhakkak et al. (2021), Kohl et al. (1997), Ruthven (1984), Rousseau (1987), Seader et al. (2011), BASF (2021), OIM Chemical (2022)

Physical properties	**Type of adsorbent**		
	Silica gel	Activated alumina	Molecular-sieve zeolites
Particle shape	Spherical or granular	Granular	Cylindrical pellets
Bulk density, ρ ($kg \cdot m^{-3}$)	720	769-871	640-720
Average porosity, ε (%)	50-65	50	60
Regeneration temperature (°C)	150-260	175-260	200-250
Surface area, S_g ($m^2 \cdot g^{-1}$)	750	320	-
Pore diameter, d_p (nm)	2-20	1.0-7.5	0.3-1.0
Pore distribution, V_p ($cm^3 \cdot g^{-1}$)	0.40	0.40	0.30
Heat of adsorption ($kJ \cdot kg_{H2O}^{-1}$)	2512	2890	4187
Dew point (°C)	-60	-40	-100
Specific heat capacity, C_p ($kJ \cdot kg^{-1} \cdot K^{-1}$)	0.921	1.005	0.963

In PSA, due to no heating or cooling of the bed being required between the adsorption and desorption (purge) steps, the duration of the cycles may be very short (Kohl *et al.*, 1997). Various modifications to the Skarstrom cycle can be made, usually adding further depressurization, pressurization and equalization steps, in order to increase hydrogen recovery and purity.

The first modification over this process was the introduction of a pressure equalization step after the purge and adsorption steps. Instead of depressurizing directly the second column after adsorption, it is connected to the first column, which just has been purged, in order to equalize the pressure. This additional step conserves energy as the compressed gas at high pressure is used to pressurize the low-pressure column. In addition, losses from the depressurization step are reduced, improving recovery of the light component (Ruthven *et al.*, 1994).

In the specific case of hydrogen drying, it is also recommended to include recycling of the wet hydrogen back to the fresh column to improve recovery. This operation requires the treatment of the gas, including its compression to the inlet pressure with subsequent cooling down and removing excess water through a gas-liquid separator (Ligen *et al.*, 2020).

2.2.2 Vacuum Pressure Swing Adsorption

A variation of the PSA process includes the implementation of a vacuum pump in the off-gas stream. While in PSA the purging step is carried out at atmospheric pressure, in Vacuum Pressure Swing Adsorption (VPSA), purging is complemented by vacuum in order to better desorb impurities with strong adsorption capacity from the adsorbent. This is translated in fewer losses of the light component, greater regeneration of the column and, consequently, an increase in the process efficiency for the same product purity and operating pressure (Ruthven *et al.*, 1994). However, there is an increase in the capital cost associated with the vacuum pump (Ruthven, 1984). A schematic diagram of a two-bed VPSA cycle is presented in Figure 2.5.

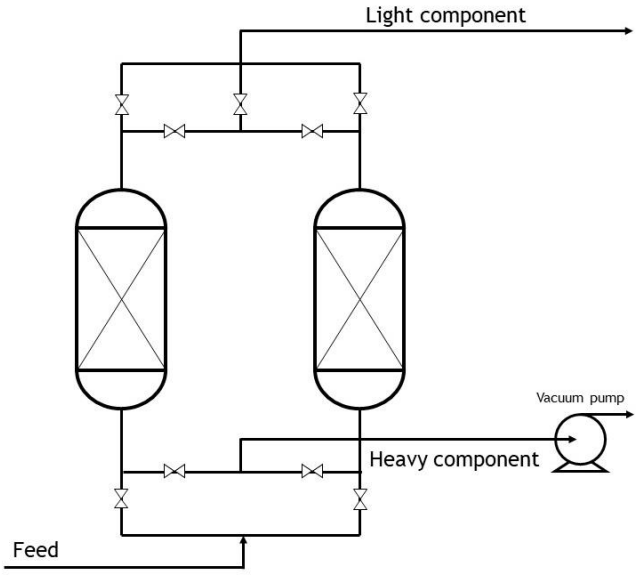

Figure 2.5 - Schematic diagram of a basic VPSA cycle.

Amnis Pura recently achieved 90 % of recovery using this approach. In literature, a VPSA system operating at 35-38 bar was reported achieving a recovery of 98.4% with a water content of less than 0.1 ppm and an energy consumption of only 0.5 $kWh \cdot kg_{H2}$. This was possible because 75% of the waste gas was recycled and used a very small purging flow (Ligen *et al.*, 2020).

2.2.3 Temperature Swing Adsorption

Another variant of the PSA process takes advantage of the exothermic nature of the adsorption phenomenon, which means that a decrease in temperature promotes the adsorption of the heavy component while an increase favours the regeneration of the adsorbent. This fact infers that a heating step improves the regeneration efficiency (Kohl *et al.*, 1997). Temperature Swing Adsorption (TSA) consists of an adsorption step at a relatively low/ambient temperature followed by the bed being purged at an increasing temperature. Then, the cooling is achieved passively or using a cooling fluid before column is ready to start the new adsorption step. TSA requires high energy consumption for the heating stage and is more time consuming than PSA due to the heating and cooling cycles. For this reason, TSA is commonly used for gas dehydration and for the removal of small concentrations of strongly adsorbed impurities (Golmakani, 2017). A simple two-bed TSA cycle is presented in Figure 2.6.

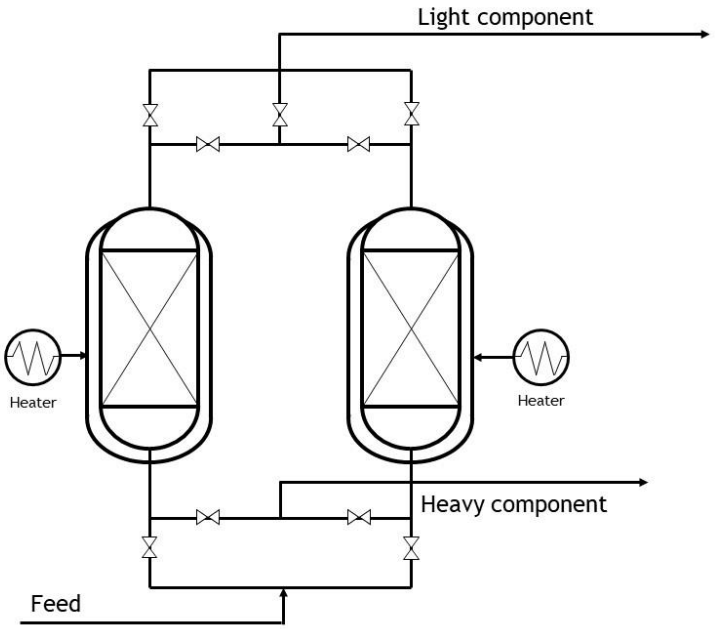

Figure 2.6 – Schematic diagram of a basic TSA cycle.

Depending on the specific application, desired purity, production capacity and operating conditions, the choice of method may differ. Despite TSA typically allowing a better regeneration of the adsorbent than PSA, it is associated with higher operating costs. On the other hand, VPSA usually allows for lower energy costs and higher productivity, but the capital investment is significantly increased. For hydrogen purification, the three processes are applicable when considering the factors mentioned above and are all considered in this study.

2.3 Economic analysis

The assessment of the economic aspect of the systems is essential, not only to evaluate the best alternative available and its feasibility, but also to encourage the implementing of these initiatives. Therefore, the main goal of the economic analysis is to evaluate all possible scenarios in order to determine the most advantageous in terms of both technical and economic aspects. For that purpose, the hydrogen purification and its capital and operating costs are investigated and economic performance indicators are measured.

2.3.1 Total Capital Investment

Capital investment can be simply described as the total cost of designing, constructing and installing a plant. It includes all physical assets of the process, including machinery, buildings and land. The capital required for manufacturing and facilities is designated fixed-capital investment (FCI) and for the operation is called working capital (WC), the sum of both is the total capital investment (TCI).

Fixed-capital investments (FCI) are divided into direct and indirect costs, which refer to manufacturing and nonmanufacturing costs, respectively. The cost of the equipment required is the basis for estimates of direct costs, taking into consideration the purchased equipment and its installation, the instrumentation and controls required, piping, electrical systems, buildings, land and service facilities. Although the most accurate way to determine equipment costs is directly through the suppliers, an estimation can be obtained by using the six-tenths factor rule, which uses the cost of an existing equipment and the size or capacity for the required unit. On the other hand, indirect costs account for all the components that are not directly related to the process itself, which include engineering, supervision and construction expenses, legal and contractors' fees and contingencies.

Working Capital (WC) accounts for the total amount invested in raw materials, supplies and products in stock as well as receivable or payable accounts and taxes. These usually refer to the equivalent of 1 month of production and for chemical plants typically represent 10 to 20% of the initial total capital investment (TCI) (Seider *et al.*, 2003).

2.3.2 Operating Costs

Operating costs take into account variable production costs, fixed charges and plant overhead costs. Fixed operational costs include equipment maintenance, labour and taxation, while the variable costs account for raw materials and utilities costs.

An aspect to consider in the fixed operational costs is the operating labour. It can be divided into skilled and unskilled labour and the number of required workers varies based on the type

of equipment and plant capacity. Other fixed costs include the depreciation of the equipment and other material objects, the interest rate of borrowed capital and insurance.

In the chemical industry, the variable production costs are mainly owed to the raw materials used in the process and can account for 10 to 60% of the total product cost. Through material balances, the amount of raw material to be supplied can be obtained by unit of time or product. Additionally, utility requirements are determined from material and energy balances and its cost depends on the amount needed, as well as its source and the location of the plant (31-Peters *et al.*, 2003).

2.3.3 Economic measures

In order to calculate profitability, different methods can be used. Levelized Cost of Electricity (LCOE) is an economic measure that allows determining the cost of energy over the lifespan of the project and comparing it across various technologies and/or projects. It relates the costs generated by the system with the amount of energy the system can produce (Delapedra-Silva *et al.*, 2022). Additionally, a similar approach for hydrogen is possible. Levelized Cost of Hydrogen (LCOH) allows an estimation of how much it costs to produce hydrogen, depending on its capital investment, operating costs and production over a time period. In Figure 2.7, the global LCOH for different energy sources for 2019 and an estimation for 2050 are presented (Leiblein *et al.*, 2021).

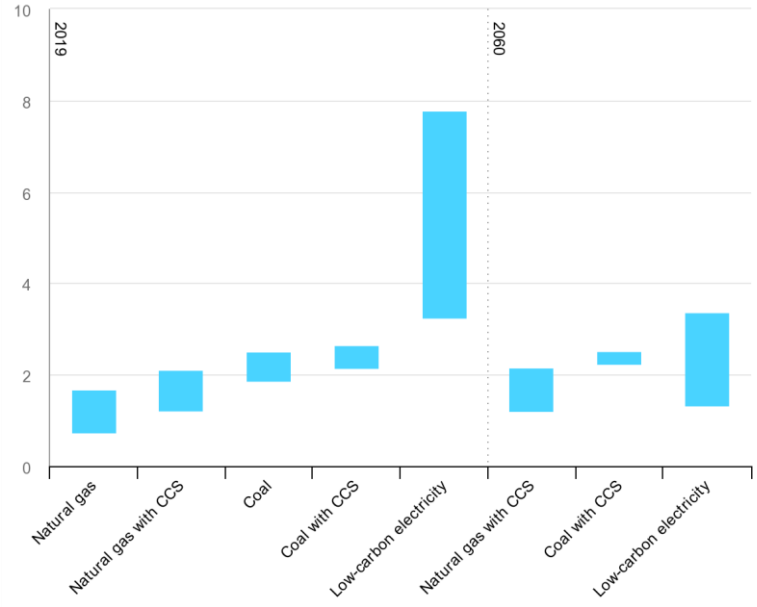

Figure 2.7 - Global average levelized cost of hydrogen production by energy source and technology, 2019 and 2050. Extracted from International Energy Agency (2022).

3 Materials and Methods

3.1 Process Simulation and Assumptions

Three contaminants are likely to be found in hydrogen obtained from water electrolysis: nitrogen, oxygen and water. However, only water removal is considered in the present work, as nitrogen can usually be removed by venting the initial production and oxygen through catalytic recombination, as mentioned earlier.

A scheme of the complete system of purification of electrolytic hydrogen is presented in Figure 3.1. However, the scope of this work relies on hydrogen drying and is focused on the components inside the dashed line.

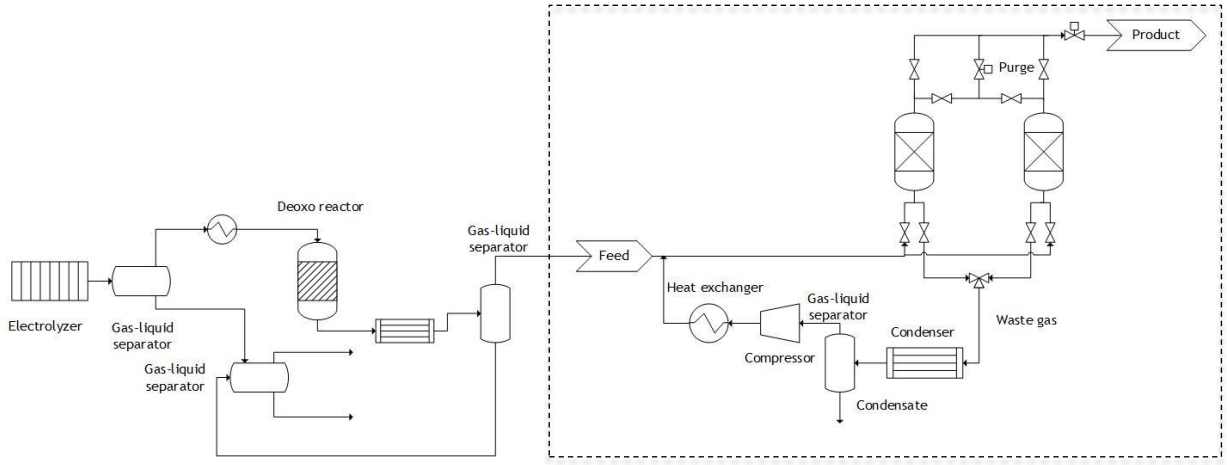

Figure 3.1 – Simplified flowsheet of hydrogen drying from an electrolyzer.

Three different methods for hydrogen drying were evaluated: PSA, VPSA and TSA. These processes were compared in terms of energy and economic costs per mass of purified hydrogen. Both energy and economic analysis were performed with support of the Aspen Plus® software. Simulations were performed considering the Peng-Robinson equation of state, which is particularly suitable for high temperature and high pressure operations, and the Peng-Robinson-Redlich-Kwong equation of state, which fits best for mixtures of non-polar and polar compounds in combination with light gases.

It should be noted that the dynamic simulation of the processes is out of the scope of the present study, instead, the performance (*i.e.* recovery) of the different methods was fixed based on the internal knowledge of the company as well as relevant literature. The assumed performances are further summarized in Table 4.1 and are based on processes designed to achieve a dew point of -66 °C.

In PSA, hydrogen recovery typically ranges 70 to 75% (Bexiga, 2021), whose low recovery is attributed to the purging gas and depressurization losses. In its turn, due to regeneration under vacuum, VPSA can achieve higher recovery thanks to the decrease in the purge to feed ratio. In this case, 90 % recovery was assumed. Additionally, in the case of TSA, a purge-to-feed ratio of 15 % was considered.

The product from water electrolysis is the feed stream for the purification process and so the inlet conditions of the gas correspond to the operating conditions of electrolysis, which correspond to a pressure of 30 bar and temperature of 40 °C. The feed consists of saturated hydrogen, which for these conditions, is 2462 ppm of water. To meet ISO levels, water needs to be reduced to a maximum of 5 ppm.

Because the wet hydrogen is already at high pressure, no pressurization is required for the feed. In PSA, the cycle includes adsorption, purge and depressurization. A previous study showed that the cycle time is not significant for the water adsorption in activated alumina within the range of 100 to 180 seconds (Pinto, 2022). For this reason, it was considered that a total cycle time of 2 minutes is sufficient to achieve the target recovery. Due to the vacuum regeneration step, the VPSA cycle may take longer and a duration of 10 minutes was assumed, according to a recent study (Ligen *et al.*, 2020). TSA is significantly slower than the other processes, owing it to the heating and cooling steps. High temperature should be achieved in order to assure the adsorbent regeneration, which also implies greater cooling. This process commonly lasts over an hour and 8 to 12 hours per cycle are suggested (Ruthven *et al.*, 1994), although in this study 4 hours were considered.

Based on the company's internal knowledge, the dimensions of the adsorption columns were defined, for obtaining the mass of adsorbent and the volume of the columns. Activated alumina was chosen as the adsorbent for the PSA system. The mass of adsorbent was estimated taking into account the water vapor effective adsorption isotherms obtained by Ferreira *et al* (2011).

3.2 Systems description

3.2.1 Base Case

In a PSA system, a hydrogen stream, obtained from water electrolysis, at about 40°C and 30 bar, enters the column at a flow rate of 60 $Nm^3 \cdot h^{-1}$. To meet ISO levels, water needs to be reduced to a maximum of 5 ppm.

In the PSA, the water is adsorbed and dry hydrogen leaves through the top of the column. After that, the column is depressurized, and dry hydrogen obtained in the other column is used for purging. The remaining gas and the desorbed water are discharged from the column, resulting in hydrogen losses.

Since hydrogen is electrochemically pressurized in the electrolyzer (before the PSA), the PSA process operates with practically no power consumption, as the energy required in only for the control electronics. In its turn, VPSA requires energy for operating the vacuum pump, while TSA has a more significant impact due to the column heating. Still, it should be noted all three processes have energy losses related to the hydrogen lost through waste gas, which has important energy value. When waste gas is entirely recycled, the energy loss associated to hydrogen is mitigated. However, to be recycled, the waste gas needs to be treated, which has energy associated to with the condensers, in addition to the equipment costs.

3.2.2 PSA with recycling

This system includes a simple PSA system with a recycling step, shown by the process flow diagram in Figure 3.2.

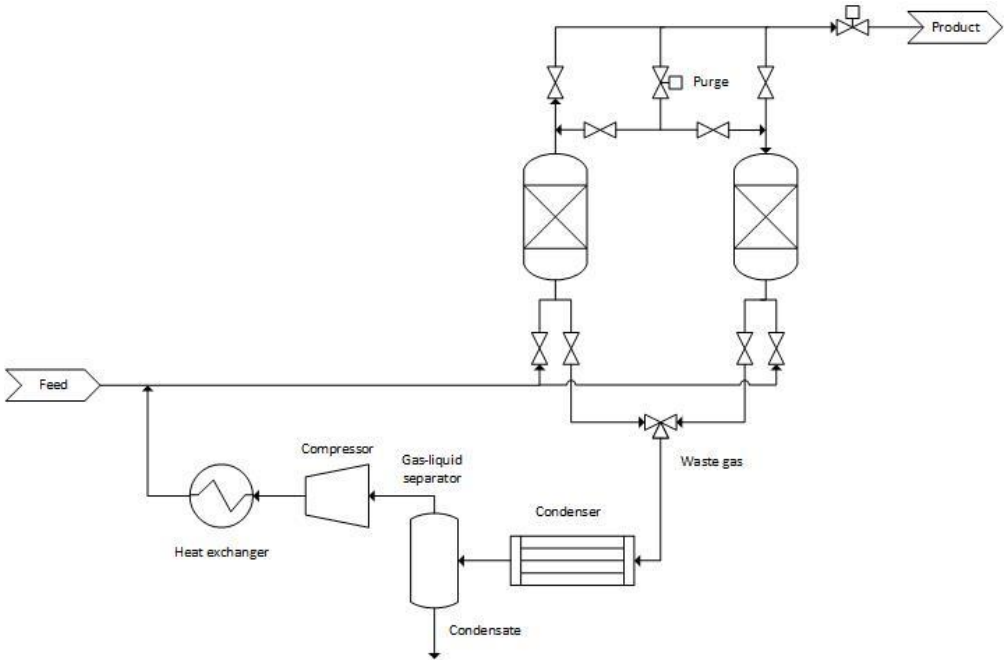

Figure 3.2 – Flowsheet of the PSA system with recycle.

As the adsorption stage occurs at 30 bar, pure hydrogen is produced at nearly the same 30 bar. The waste gas is released during the blowdown (depressurization) and purge steps, at atmospheric pressure and it is further re-compressed to 30 bar for recycling to the feed stream.

As the pressure increases in the compressor, high temperature is reached and a heat exchanger needs to be coupled to the compressor. Otherwise, the temperature achieved through an isentropic process could range the 600 to 800ºC.

3.2.3 VPSA with recycling

In this system, the main difference is the addition of vacuum in the waste gas. Similarly to the PSA process, recompression, cooling and water condensates removal are required for the recycling.

After adsorption, the column is depressurized and waste gas is evacuated. Discharge temperature of vacuum pumps is typically around 85 ºC, which is higher than the recommended operating temperature of the compressor. Therefore, two heat exchangers were considered, one before and one after the compressor. Because the outlet of the vacuum pump is at atmospheric pressure, the dew point of the gas is low, hence the need of a refrigerator to condensate the water for further removal in a gas-liquid separation. The temperature of the condenser was defined to achieve a relative humidity of 95 % after the compressor. After being compressed, the gas is refrigerated to the operating temperature, before being recycled into the next column. This configuration is shown in Figure 3.3.

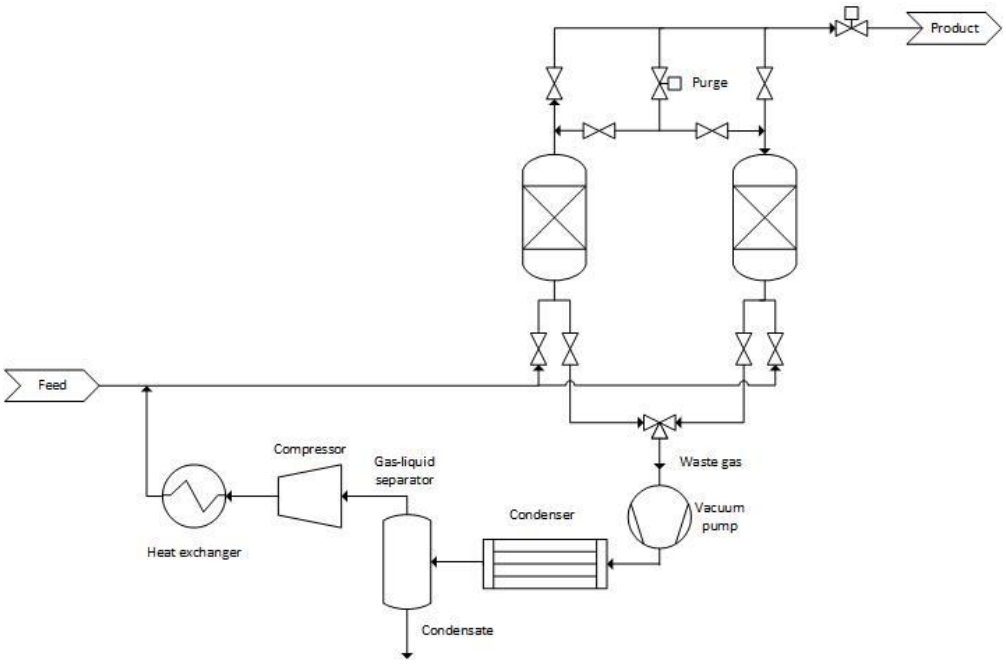

Figure 3.3 – Flowsheet of the VPSA system with recycle.

3.2.4 TSA with recycling

Contrarily to PSA and VPSA, the waste gas does not require a high recompression stage to be recycled. Instead, a small blower is installed in purge line, with the objective to surpass the pressure drop in the system, thus allowing gas recirculation. In this case, the blower was sized to increase the pressure by 300 mbar.

In the regeneration stage a jacketed heater is used to increase the temperature of the column and favour desorption. The posterior cooling of the column for adsorption step was considered passive, which means it does not require additional energy or equipment. The regenerating temperature was assumed to be 200 °C. The whole process is represented in Figure 3.4.

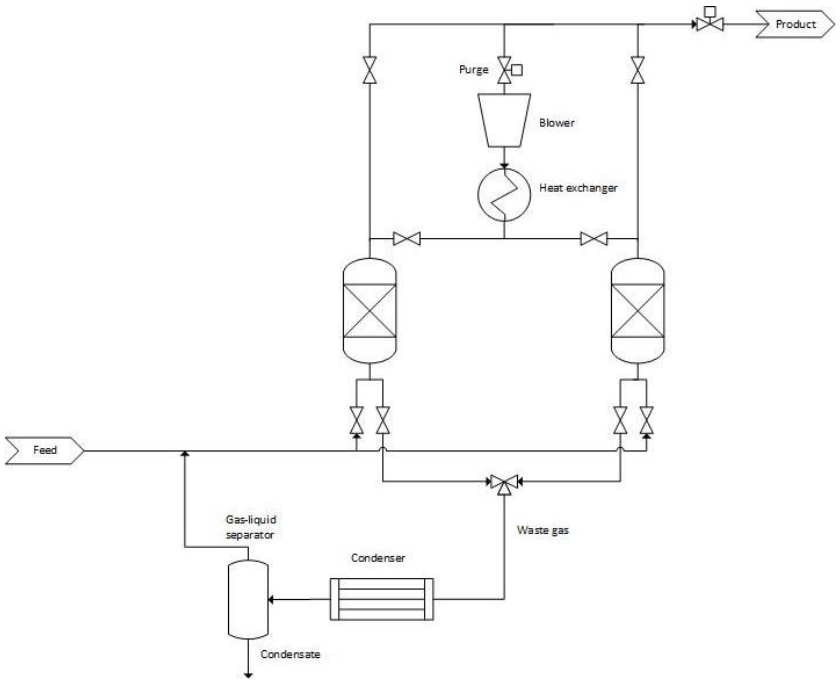

Figure 3.4 – Flowsheet of the TSA system with recycle.

3.2.5 Different scenarios

Different operating pressures (20, 30 and 40 bar) were studied in order to determine the most cost-effective option for each method. It should be noted that for different pressures, hydrogen saturation is achieved at different temperatures, resulting into different water content.

Different flow rates were also evaluated for those same pressure conditions, in order to enquire whether the same efficiency results would be obtained for a laboratory scale and a larger scale. The volume of gas in the columns significantly changes and the dimensions need to be modified. The ratio between column length and diameter (L/D) was kept the same in all scenarios for the sake of simplicity, which was based on a recent VPSA study (Ligen *et al.*, 2020). The exception

was made for the 20 000 $Nm^3 \cdot h^{-1}$ case, in which the L/D was reduced to keep a maximum column height of 5.0 meters.

Mass of adsorbent was initially estimated based on the adsorption equilibrium isotherms obtained by Ferreira *et al* (2011). The working capacity of the adsorbent material was assumed 10% of the total adsorption capacity. Specifications for the different beds are presented in Table 3.1.

Table 3.1 - Specifications of the adsorption beds for different flow rates.

Flow rate	$Nm^3 \cdot h^{-1}$	**5**	**60**	**200**	**20000**
Internal diameter	m	0.09	0.20	0.31	1.96
Length	m	0.60	1.37	2.04	5.00
Mass of adsorbent	kg	2.90	34.80	116.01	11601
Bed porosity	-	0.40			
Wall density	$kg \cdot m^{-3}$	790			
Wall specific heat	$J \cdot kg^{-1} \cdot K^{-1}$	460			

3.3 Economic analysis

An analysis of the costs associated with the process is necessary in order to select the best available option, taking into consideration both process equipment and operation conditions. Economic analysis is utilized to evaluate the profitability of all the different scenarios and select the one with greater technical and economic advantages.

3.3.1 Total Capital Investment

Capital investment estimates may vary depending on the detail of the information available. In this work, a study estimate was used, which is based on the knowledge of major items of equipment and has an accuracy range of about 30% (Peters *et al.*, 2003).

The Total Capital Investment (TCI) is determined based on the cost of the purchased equipment and takes into account the ratio between the current and the base Chemical Engineering Plant Cost Index (CEPCI). The CEPCI base value is 394, which is the value for the year 2000, and the current CEPCI value is 821, as of September 2022 (Towering Skills, 2023).

In general, to estimate the purchase cost, the capacity of the equipment and a material factor are considered. The correlations used to estimate the cost of purchased equipment are described in further detail in Appendix B (Seider *et al.*, 2003).

Other costs included in the TCI are generally obtained by an average of their typical contributions, except for land and buildings, which take the smallest value, as the plant in study would be relatively small, when compared to typical industrial chemical plants.

3.3.2 Operating Costs

The operating costs include the variable production costs, which account for utilities (electricity and cooling water) and raw materials (hydrogen from electrolysis). Electricity was considered to cost 0.07 €·kWh^{-1} (International Energy Agency, 2020) and the cooling water 1.78 €·m^{-3} (Águas do Porto, 2023).

The fixed production costs take into consideration adsorbents, equipment maintenance and other costs associated with the operation of the plant and are estimated based on material and energy balances. The skilled labour is included in the equipment maintenance while the operating labour depends on the requirements for each process equipment. Some of the relevant values for the processes under study are presented in Table 3.2. Additionally, the plant overhead costs are part of the operating costs, and these include general expenses such as administrative, marketing, distribution and research and development expenses (Peters *et al.*, 2003).

Table 3.2 - Typical labor requirements for process equipment. Adapted from Peters et al. (2003).

Type of Equipment	Workers/unit/shift
Compressor	0.1-0.2
Heat exchanger	0.1
Process vessels	0.2-0.5

It was assumed an annual salary of 30000€ for these workers, and because a continuous production (of 24 hours a day) was considered, 3 shifts were necessary. Additionally, the economic analysis assumes 340 days in a year of continuous operation, a plant lifetime of 10 years (and none of the equipment is replaced in that time period) and an interest rate of 5%.

3.3.3 Economic Measure

In order to evaluate the economic feasibility of these projects, the Levelized Cost of Electricity (LCOE) was determined, using Equation 3.1 (Corporate Finance Institute, 2022).

$$LCOE = \frac{I_0 + \sum_{t=1}^{n} \frac{I_t + E_t + M_t}{(1+r)^t}}{\sum_{t=1}^{n} \frac{F_t}{(1+r)^t}} \quad (3.1)$$

In this equation, I_t corresponds to the investment expenditures in year t, M_t is the operations and maintenance expenditures and E_t represents the energy expenditures. The number of the year is t and the discount rate is r. F_t indicates the electricity generation through the hydrogen purified, by the system in the year t.

4 Results and discussion

This section presents the results obtained for the different scenarios, which were analyzed with reference to the energy consumed by the amount of hydrogen produced. The energy consumed includes electrical energy for the equipment operation and the energy wasted through losses of hydrogen through the process, which was considered as 33.33 $kWh \cdot kg^{-1}$ of usable energy (IDEALHY, n.d.). In order to achieve the highest hydrogen recovery, all waste gas must be recycled, releasing only water as waste. However, this is the most energy-intensive part of the process and the overall energy and economic costs are compared.

4.1 Base Case

In order to examine whether recycling reduces total energy consumption, a preliminary study of the total energy loss of the systems without recycling must be attained. For this purpose, the consumed operation energy and the wasted energy through hydrogen losses were calculated in terms of mass of hydrogen purified and are presented in Table 4.1. These values refer to the base system, operating at 30 bar and a feed of 60 $Nm^3 \cdot h^{-1}$. As it can be observed, the PSA presents the lowest energy consumption amongst the three processes, while TSA is the system with the highest energy consumption. However, when the energy associated with the lost hydrogen is taken into account, VPSA is the system with the most favorable choice. Accordingly, the system performance should consider not only the hydrogen recovery and energy consumption but also the energy value of the lost hydrogen. In the case of TSA, commercial systems typically include a recirculation, which makes it the most obvious choice if recirculation is not considered for PSA or VPSA.

Table 4.1 – Energy consumed by systems without recycling.

	Units	PSA	VPSA	TSA
Recovery	%	75	90	85
Energy consumed	$kWh \cdot kg^{-1}$	0	0.057	0.293
Energy associated to lost H_2	$kWh \cdot kg^{-1}$	12.924	5.295	7.539

Moreover, for the PSA and VPSA systems without recycling to be competitive with the typical TSA system and consume similar amount of energy per mass of hydrogen purified, these would need to operate with a recovery rate of 98.4%. These processes do not allow such high recovery and for this reason, the recycling step should be implemented to reduce energy consumption.

4.2 Pressure Swing Adsorption

In Table 4.2, the flows corresponding to the inlets and outlets of the columns for a feed flow rate of 60 $Nm^3 \cdot h^{-1}$ and operating at the designated pressure, are presented. The amount of water removed from the waste gas before being recycled is also included.

Table 4.2 – Mass flows in a PSA two-bed system.

Operating pressure	bar	20	30	40
Feed flow rate	$Nm^3 \cdot h^{-1}$	60		
Feed	$kg \cdot h^{-1}$	5.555	5.502	5.476
Product	$kg \cdot h^{-1}$	5.041	5.067	5.100
Recycle	$kg \cdot h^{-1}$	1.656	1.553	1.502
Water removed	$kg \cdot h^{-1}$	0.513	0.435	0.376

After leaving the column, the gas requires compression and cooling. Two configurations for this process were studied: Configuration A, which consists in compressing the stream and then cooling it to the operating temperature; and Configuration B (Figure 3.2), in which the gas is cooled and excess water is removed before being compressed. The power required for each configuration is compared and shown in Figure 4.1. As it can be observed, configuration B is the most efficient configuration from the energy point of view. However, in this configuration an extra heat exchanger (HEATX) is needed and the energy consumption of the condenser (COND) is higher, because the water is removed at low pressure (lower dew point). The overall reduction in the energy consumption is explained by the lower water content in the compressor.

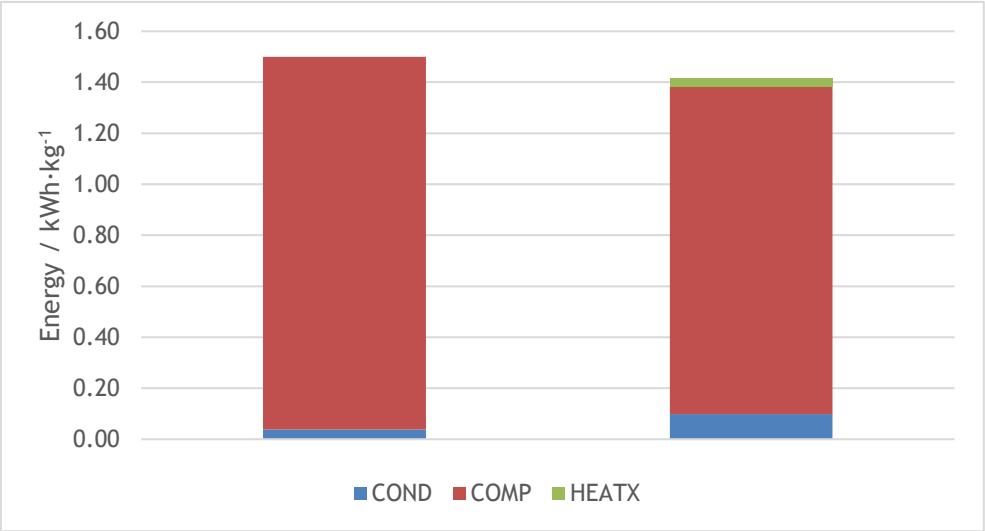

Figure 4.1 - Energy required per mass of hydrogen purified for two configurations for PSA with operating pressure of 30 bar.

Figure 4.2 depicts the energy required for operating at different pressures, whose values are summarized in Table 4.3. The results reinforce that the compressor has the major contribution for the power consumption of the system, which increases with the operating pressure increase. The same stands for the condenser, the higher the pressure the higher the energy consumption, because to achieve 95 % of relative humidity after the compressor, a lower dewpoint is required in the condenser. A temperature of -6.8 °C, -11.4 °C and -14.5 °C must be reached for an operating pressure of 20, 30 and 40 bar, respectively. The opposite trend is observed for the heat exchanger after the compressor, which requires less energy because the quantity of water in the recirculating stream is lower. Although the lower operating pressure is the best configuration from the purification point of view, consuming a total of 1.192 kWh·kg^{-1} compared to the 1.594 kWh·kg^{-1} for the 40 bar, this should be further analyzed in the overall system, in which a downstream compression stage up to 200, 350 or 700 bar is typically considered.

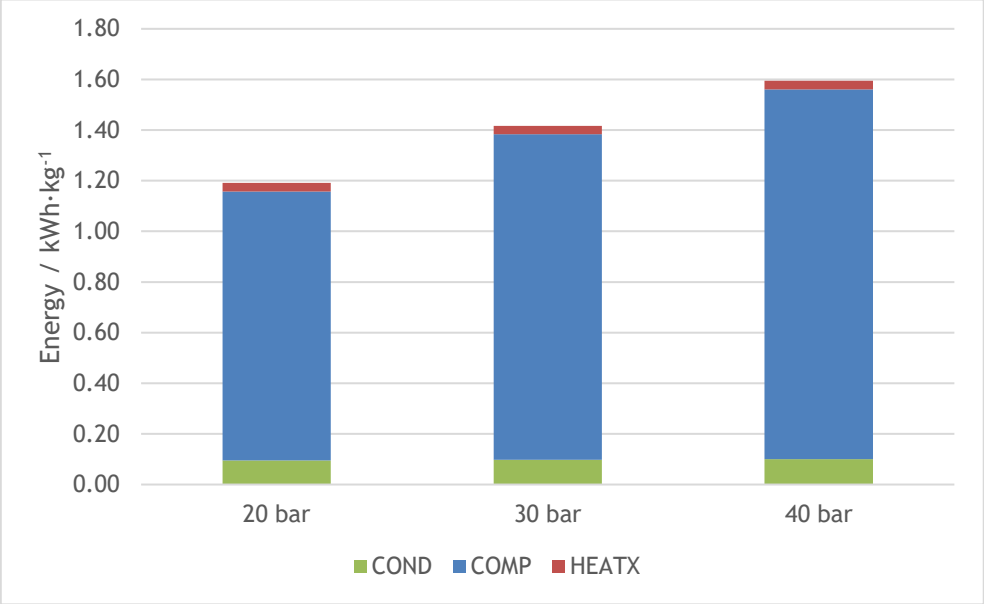

Figure 4.2 - Energy consumption per mass of hydrogen purified for recycling in PSA operating at 20, 30 and 40 bar.

Table 4.3 - Energy requirements of a PSA system for pressures of 20, 30 and 40 bar.

Pressure	bar	20	30	40
Condenser energy	kWh·kg^{-1}	0.095	0.098	0.101
Compressor energy	kWh·kg^{-1}	1.063	1.285	1.460
Heat exchanger energy	kWh·kg^{-1}	0.034	0.034	0.033
Total energy required	**kWh·kg^{-1}**	**1.192**	**1.417**	**1.594**

4.3 Vacuum Pressure Swing Adsorption

For the VPSA system, the most significant difference to the PSA in terms of flow is the higher recovery, which translates in less recirculating gas. The corresponding flow rates are presented in Table 4.4, for pressures of 20, 30 and 40 bar.

Table 4.4 – Mass flows in a VPSA two-bed system.

Operating pressure	bar	20	30	40
Feed flow rate	$Nm^3 \cdot h^{-1}$	60		
Feed	$kg \cdot h^{-1}$	5.555	5.502	5.476
Product	$kg \cdot h^{-1}$	5.283	5.288	5.299
Recycle	$kg \cdot h^{-1}$	0.876	0.763	0.707
Water removed	$kg \cdot h^{-1}$	0.271	0.214	0.177

During the VPSA cycle, the stream is evacuated by the vacuum pump, whose outlet is at atmospheric pressure. Then, the waste gas is pressurized to the operating pressure. Like in the PSA case, two configurations were considered: Configuration A, consisting of a compression stage after the vacuum pump, followed by cooling to the operating temperature; and Configuration B (Figure 3.3) in which the gas is cooled and excess water is removed between the vacuum pump and the compressor. The results are presented in

Figure 4.3.

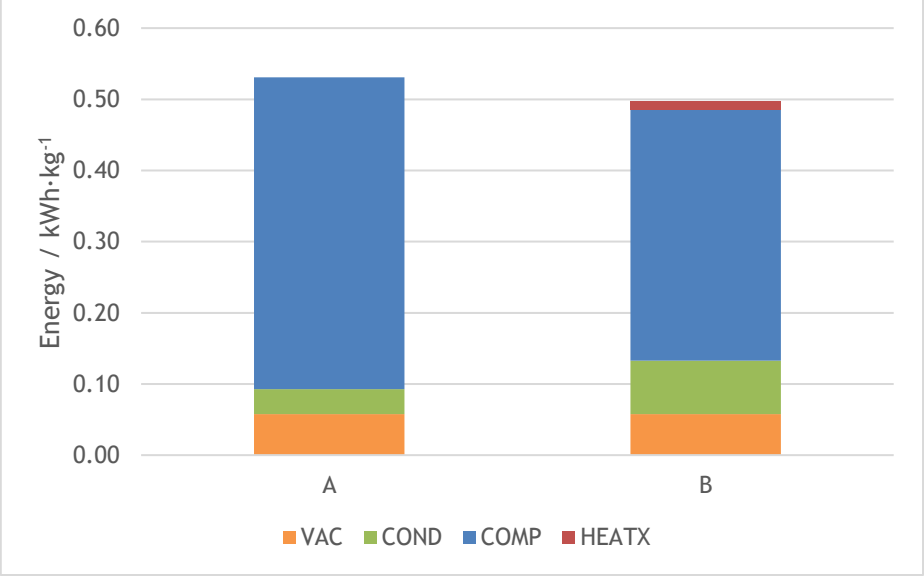

Figure 4.3 - Energy required per mass of hydrogen purified for configurations for VPSA with operating pressure of 30 bar.

The same conclusions taken for the PSA case can be drawn for the VPSA: Configuration (B) is the most efficient because of the lower power requirement for the compression stage due to the lower water content. However, while in the PSA the energy consumption of the condenser is higher for higher pressure, the opposite is observed for the VPSA. The slight difference in the vacuum pump consumption is explained by the higher water content at lower pressures, due to the higher dewpoint. Figure 4.4 and Table 4.5 summarize the energy requirements of the different equipment for the VPSA case and show that the energy consumption accounts for 0.449 kWh·kg^{-1} at 20 bar while at 40 bar 0.536 kWh·kg^{-1} are consumed.

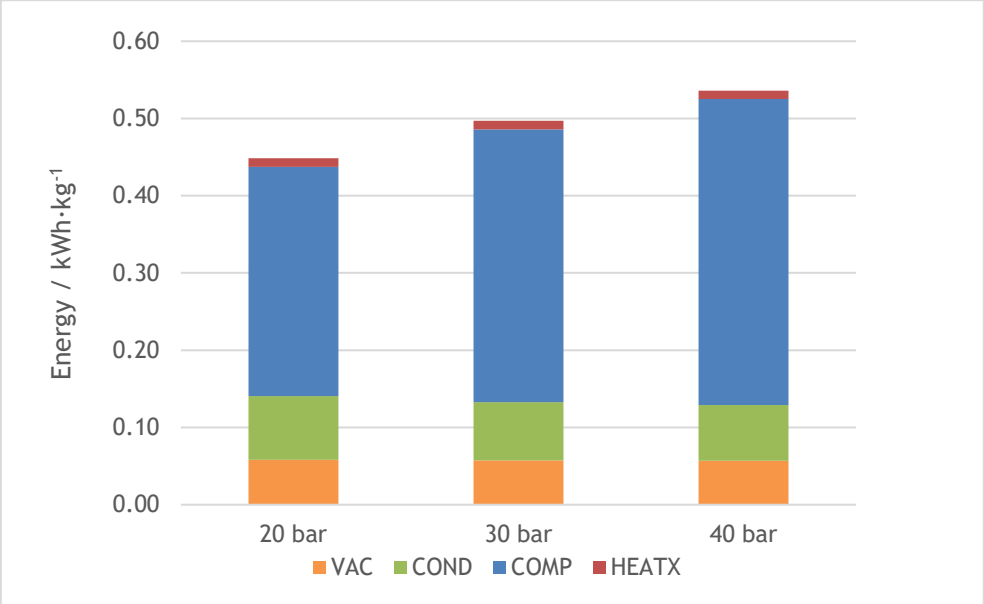

Figure 4.4 - Energy consumption per mass of hydrogen purified for recycling in VPSA operating at 20, 30 and 40 bar.

Table 4.5 - Energy requirements of a VPSA system for pressures of 20, 30 and 40 bar.

Pressure	bar	20	30	40
Vacuum pump energy	kWh·kg^{-1}	0.058	0.057	0.057
Condenser energy	kWh·kg^{-1}	0.082	0.075	0.072
Compressor energy	kWh·kg^{-1}	0.297	0.353	0.396
Heat exchanger energy	kWh·kg^{-1}	0.011	0.011	0.011
Total energy required	kWh·kg^{-1}	**0.449**	**0.497**	**0.536**

4.4 Temperature Swing Adsorption

The flow rates of a TSA system designed to treat 60 $Nm^3 \cdot h^{-1}$ are shown in Table 4.6.

Table 4.6 – Mass flows in a TSA two-bed system.

Operating pressure	bar	20	30	40
Feed flow rate	$Nm^3 \cdot h^{-1}$	60		
Feed	$kg \cdot h^{-1}$	5.555	5.502	5.476
Product	$kg \cdot h^{-1}$	5.203	5.215	5.233
Recycle	$kg \cdot h^{-1}$	1.135	1.027	0.972
Water removed	$kg \cdot h^{-1}$	0.352	0.287	0.243

In a TSA system, energy is required to heat the column and the recirculating purge gas. Because waste gas leaves the column at the operating pressure and a higher temperature, its recycling consists in cooling down the stream and remove excess water. Additionally, the purge flow is subjected to a slight pressure increase to improve desorption. With this in mind, four different units are necessary: a jacketed heater to increase the column temperature for regeneration, a heat exchanger to cool the waste gas, and finally a compressor and heater for the purge flow. The power required by these units is displayed in Figure 4.5 and Table 4.7 for the different operating pressures.

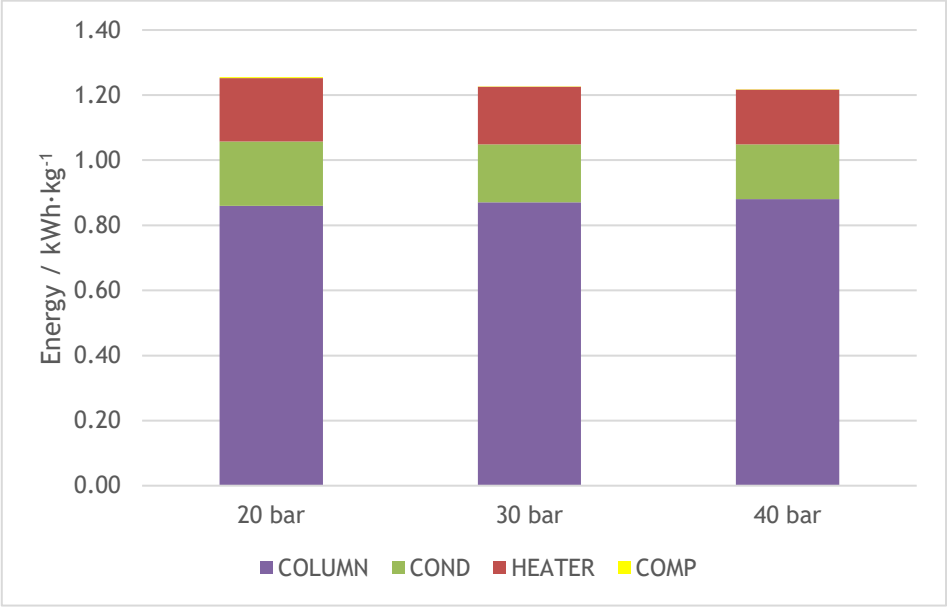

Figure 4.5 – Power consumption for recycling in TSA operating at 20, 30 and 40 bar.

The main energy cost is associated with the heating of the column, including the column wall (stainless steel), adsorbent material, and adsorbed gas, which accounts for 0.860 $kWh \cdot kg^{-1}$ at 20 bar and 0.880 $kWh \cdot kg^{-1}$ at 40 bar. Contrarily to the previous systems, energy demand for TSA decreases for increasing pressure due to the lower water content at higher pressure. The difference from 30 bar to 40 bar is lower than the difference from 20 bar to 30 bar because of the thickness increase of the column. It is also visible that the difference between the different operating pressures is not as significant as for the other systems because of the low compression requirements (0.001 to 0.003 $kWh \cdot kg^{-1}$).

Table 4.7 – Energy requirements of a TSA system for pressures of 20, 30 and 40 bar.

Pressure	bar	20	30	40
Column heater energy	$kWh \cdot kg^{-1}$	0.860	0.870	0.880
Condenser energy	$kWh \cdot kg^{-1}$	0.197	0.178	0.169
Compressor energy	$kWh \cdot kg^{-1}$	0.003	0.002	0.001
Heater energy	$kWh \cdot kg^{-1}$	0.195	0.177	0.168
Total energy required	**$kWh \cdot kg^{-1}$**	1.255	1.227	1.218

4.4.1 Different Scenarios

For the TSA system the flow rate has an impact in the energy requirement, contrary to the PSA and VPSA cases. For instance, for a production of 5 $Nm^3 \cdot h^{-1}$, the required energy is 1.231 $kWh \cdot kg^{-1}$, while for 20000 $Nm^3 \cdot h^{-1}$ 1.254 $kWh \cdot kg^{-1}$ needed. This difference is related to the heating of the column, which is a function of the thickness of the columns and increases with the diameter and pressure. The assumed values were calculated by the Mechanical Department of Amnis Pura, whose values are summarized in Appendix B. **Error! Reference source not found.** summarizes the energy necessary per mass of product for each configuration and the total is shown in Table 4.8.

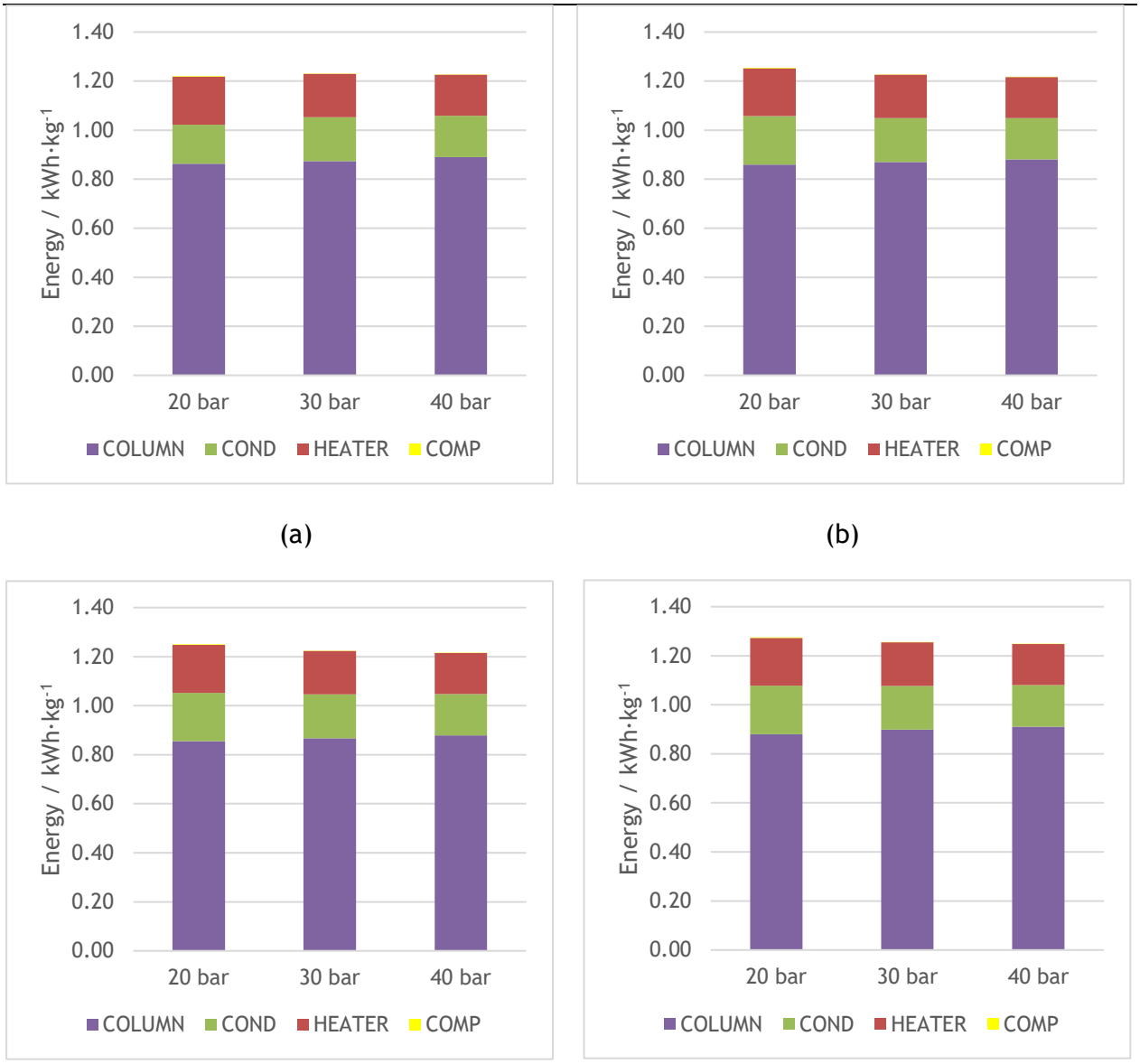

Figure 4.6 - Energy consumption for a TSA system with different operating pressures and a flow rate of a) 5 $Nm^3 \cdot h^{-1}$, b) 60 $Nm^3 \cdot h^{-1}$, c) 200 $Nm^3 \cdot h^{-1}$ and d) 20000 $Nm^3 \cdot h^{-1}$.

Table 4.8 - Total energy requirements for TSA configurations.

Pressure	bar	20	30	40
Energy for 5 $Nm^3 \cdot h^{-1}$	$kWh \cdot kg^{-1}$	1.220	1.231	1.227
Energy for 60 $Nm^3 \cdot h^{-1}$	$kWh \cdot kg^{-1}$	1.255	1.227	1.218
Energy for 200 $Nm^3 \cdot h^{-1}$	$kWh \cdot kg^{-1}$	1.250	1.224	1.216
Energy for 20000 $Nm^3 \cdot h^{-1}$	$kWh \cdot kg^{-1}$	1.275	1.254	1.247

4.5 Comparison of the different methods

Firstly, a comparison of the systems with and without recycling is summarized in Table 4.9. These results refer to a feed flow rate of 60 $Nm^3 \cdot h^{-1}$, an operating pressure of 20 bar and the recycling flow rates considered above for each process.

*Table 4.9 - Energy consumed by the systems with and without recycling for base case. *Includes the energy loss associated to hydrogen.*

	Units	PSA	VPSA	TSA
Production per cycle	kg	0.134	0.863	18.278
Production per day	kg	96.792	124.235	109.669
Energy consumed without recycling*	$kWh \cdot kg^{-1}$	13.797	5.740	8.658
Energy consumed with recycling	$kWh \cdot kg^{-1}$	1.192	0.449	1.255

It is noticeable that the recycling step allows reducing ca. 90 % of the energy consumption. This means that recycling the waste gas is indeed the best alternative to reduce energy consumption and improve hydrogen recovery. For both cases, with and without recycling, VPSA is the least energy intensive method, which is due to the fact that more hydrogen is recovered. However, when considering the same recovery for the three systems (the stream to be recycled is identical), these observations may change. These hypothetical scenarios are compared in Figure 4.7, where different recoveries (recirculating quantities) were assumed.

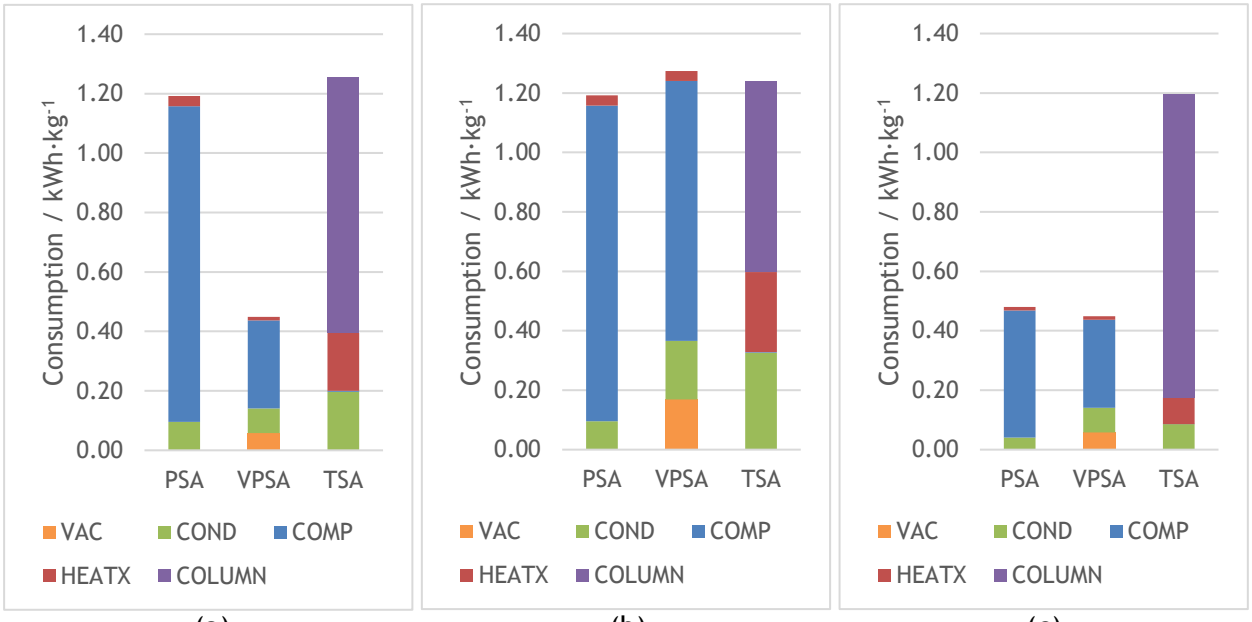

Figure 4.7 - Energy consumption for recovery rate a) PSA: 75 %, VPSA: 90 %, TSA: 85 %, b) of 75% and c) of 90%.

When considering a lower recovery (case B), a larger recycling stream will be treated, which results in increasing energy requirements. In this case, TSA presents lower energy consumption as this also means that a larger quantity of gas at regeneration temperature is fed to the column, and consequently less energy is required to heat it.

However, for the highest recovery, TSA presents the highest energy consumption amongst the different cases. This is the scenario where all three, PSA, VPSA and TSA, consume the least energy per mass of hydrogen purified. Yet, reaching such high recoveries while maintaining the purity is unlikely to happen in the case of PSA at the light of current commercially available materials. Currently, only VPSA should be considered under these conditions, making it the most energy efficient.

4.6 Economic analysis

As mentioned before, the estimate of the TCI is based on the purchase cost of the equipment. Although some of the equipment is identical for the three systems, such as the columns, specific machinery is required for certain processes. Therefore, the first step consists of comparing the cost of purchased equipment for the three different methods. The results are shown in Figure 4.8 and refer to the base case with recycling, which corresponds to an operating pressure of 20 bar and a temperature of 40º C for a feed flow rate of 60 $Nm^3 \cdot h^{-1}$.

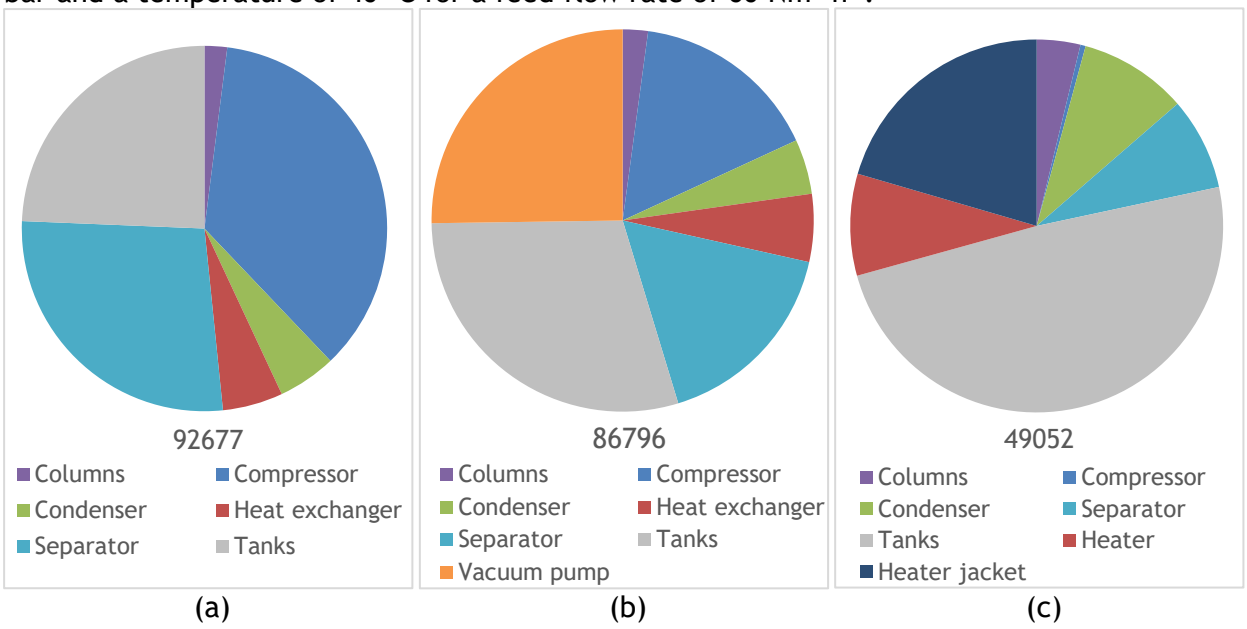

Figure 4.8 - Cost of purchased equipment for the base case for a) PSA, b) VPSA and c) TSA.

When taking into consideration that the purchase cost of the columns is similar for the three processes, it is visible that the PSA system is the most expensive in terms of equipment. The compressor, which is used in the three processes, makes a large contribution to the total cost of purchased equipment. However, for TSA, as only a small pressure increase is required, the corresponding compressor becomes very inexpensive, and most of the costs associated with this process are due to the storage tanks and the heating equipment.

After approaching the purchase cost of equipment, its installation and other factors are taken into account in order to estimate the TCI required for the process. The corresponding results are summarized in Table 4.10.

Table 4.10 – Costs associated with the Total Capital Investment for the base case.

			Contribution factor	Cost / k€		
				PSA	VPSA	TSA
Fixed Capital			**0.85**	**337.01**	**315.62**	**178.37**
	Direct			251.07	235.14	132.89
		Purchased Equipment	0.275	92.68	86.80	49.05
		Installation	0.10	33.70	31.56	17.84
		Instrumentation and Controls	0.05	16.85	15.78	8.92
		Piping	0.10	33.70	31.56	17.84
		Electrical systems	0.05	16.85	15.78	8.92
		Buildings	0.02	6.74	6.31	3.57
		Yard improvements	0.02	6.74	6.31	3.57
		Service facilities	0.12	40.44	37.87	21.40
		Land	0.01	3.37	3.16	1.78
	Indirect			85.94	80.48	45.48
		Engineering and supervision	0.1	33.70	31.56	17.84
		Legal Expenses	0.01	3.37	3.16	1.78
		Construction expenses	0.04	13.48	12.62	7.13
		Contractor's Fees	0.03	10.11	9.47	5.35
		Contingencies	0.075	25.28	23.67	13.38
	Total		1	337.01	315.62	178.37
Working Capital			**0.15**	**59.47**	**55.70**	**31.48**
Total Capital Investment			**1**	**396.48**	**371.32**	**209.85**

These results confirm that PSA requires the most capital investment, followed by VPSA and TSA, which is the least expensive in terms of capital costs. For all the scenarios considered, the lowest cost of total capital investment per mass of hydrogen produced annually corresponded to the TSA process, as expected, with a feed flow rate of 20000 $Nm^3 \cdot h^{-1}$and 40 bar of operating pressure, which resulted in a CAPEX of 0.08 €·kg^{-1} of hydrogen.

Furthermore, the operating costs are also an important factor to consider when choosing the best process and configuration. Because the hydrogen used as raw material is integrated in the overall system, it was not regarded as an expense. With that consideration, the total operating costs corresponding to the operating pressure with less energy requirements associated are presented in Table 4.11.

Table 4.11 – Operating costs per year for an operating pressure of 20 bar.

			Cost / k€		
			PSA	**VPSA**	**TSA**
Fixed Costs					
	Equipment maintenance		120.00		
	Operating Labour		6.75		
	Taxation		90.00		
Variable Costs					
	Adsorbent		0.140		
	Utilities				
		Cooling Water	0.02	0.01	0.16
		Electricity	2.67	1.21	1.07
Plant Overhead Costs			216.750		
Total Operating Costs			**436.33**	**434.85**	**436.55**

Based on these results, the yearly operating costs of the TSA and PSA are similar, while for VPSA are the lowest, which is in accordance to the energy requirements for the processes.

Considering the cost of utilities per mass of hydrogen purified, the VPSA system that purifies 20000 $Nm^3 \cdot h^{-1}$ at an operating pressure of 40 bar is the least expensive, resulting in a OPEX of 0.03 €·kg^{-1} of hydrogen. This is the expected result as the VPSA consumes the least energy per

mass purified and, despite the higher consumption of the compressor, the 40 bar system displays less amount of energy and cooling water expenditures for the remaining equipment.

Moreover, considering the total cost of the processes in study and the different types of expenses, a comparison was made in order to understand what causes the most impact in the total cost of the systems. In Figure 4.9, the costs for an operating pressure of 20 bar, the one which was deemed as the most energy efficient, are presented.

Figure 4.9 - Total cost of the plants for a) 5, b) 60, c) 200 and d) 20000 $Nm^3 \cdot h^{-1}$.

The significant contribution of the fixed operating costs for lower feed flow rates is clear. However, with increasing feed flow rate, the fixed operating costs are relatively decreasing because capital costs increase due to increasing equipment as well as operating costs related to utilities. This means that for higher flow rates, the total cost depends more on the direct costs of production and less on other expenses, resulting in lower total cost of the product.

Additionally, with increasing flow rate, the difference of total costs among the three systems becomes more evident. When taking into account both operating and capital costs, TSA displays the least total expenses per mass of hydrogen purified, with the highest flow rate and operating pressure resulting in the lowest cost per kilogram of hydrogen purified, 0.17 €·kg_{H2}^{-1}. On the other hand, PSA is the most expensive, due to the lower recovery rate, which results in less purified hydrogen but also implies more recycling and larger equipment to do so.

Furthermore, taking into consideration the lifetime of the plant, the LCOE was calculated. The minimum cost obtained for PSA, VPSA and TSA was 0.16, 0.15 and 0.14 €·kWh^{-1}, respectively, for a feed of 20000 $Nm^3 \cdot h^{-1}$ and an operating pressure of 20 bar. This also shows that TSA is the most economically efficient system, when considering the electricity produced from the purified hydrogen.

5 Conclusion

The main goal of this work was to determine the most energy and economic efficient process for hydrogen purification from electrolysis. The drying of the saturated hydrogen should reduce its water content to less than 5 ppm with maximum recovery. For that purpose, three different processes were studied, and recycling was implemented in order to avoid hydrogen losses and consequent energy waste.

A preliminary study verified that recycling reduces energy expenditures and product losses, despite the higher energy consumption. This allowed to conclude that recycling was the best approach to follow.

The subsequent configurations included two adsorption columns and the equipment required for the treatment of the recycling stream, which varied based on the process.

The energy analysis of the processes allowed to obtain the energy consumption in relation to the mass of hydrogen purified. It was possible to conclude that for the set operating conditions, VPSA was the most energy efficient method.

The effect of the operating pressure was assessed, and it was concluded that, for both PSA and VPSA, less energy was required for a lower operating pressure, due to less compression work. On the other hand, for TSA the pressure change did not significantly affect the energy consumption. Because the final required water content was achievable for all the pressures considered, it was concluded that an operating pressure of 20 bar was the best condition. For the base case, this was translated in a final energy consumption of 0.45 $kWh \cdot kg^{-1}$ using VPSA.

Additionally, the feed flow rate was considered and had the most significant impact on the economic balances of the processes. It was determined that higher flow rates have more profitability, as fixed costs are relatively smaller. Moreover, the economic analysis showed that the TSA system requires the least investment in terms of equipment and overall lowest cost per kilogram of hydrogen purified, resulting in 0.17 $€ \cdot kg_{H2}^{-1}$. When considering the chosen economic measure, it was also shown that TSA is the most economically advantageous process.

In conclusion, despite VPSA consuming less energy per quantity of product, when both energy and economics are considered, TSA is the most efficient process for hydrogen purification from electrolysis, as it requires less capital investment and operating costs.

Future work should include an experimental analysis of the proposed configurations in order to ascertain whether the estimated results are in agreement with those achieved on a laboratory and a pilot scale.

6 Assessment of the work done

6.1 Objectives Achieved

The main objective of this work was the study of a hydrogen purification system from electrolysis, which is accomplished through Pressure Swing Adsorption, Vacuum Pressure Swing Adsorption or Temperature Swing Adsorption. This objective was achieved, allowing the conclusion that recycling the off-gas stream presents an advantage in terms of energy waste.

Another objective was the energy analysis of the different purification processes, which was achieved through comparison of the different scenarios and operating conditions.

The final goal was the economic analysis of the different scenarios, which was only accomplished through a study estimate, that confers an error of about 30%.

6.2 Final Assessment

The developed work in this study firstly allowed developing a more profound knowledge in the green hydrogen sector and hydrogen as an energy-carrier.

Furthermore, I was able to learn more about hydrogen purification systems, as well as the required steps for its drying and the final requirements to be used in fuel cells. This also included a better understanding of some of the machinery used as well as the energy and economic aspects of this process.

Finally, this work convinced me that a global transition for cleaner energy is achievable, with currently the economic aspect being the main drawback. For this reason, I believe that, although there is still a long way to go, there is great potential in green hydrogen and water electrolysis as a path to sustainable energy production and consumption.

7 References

- Águas do Porto. 2023. Tarifário 2023. https://www.aguasdoporto.pt/files/uploads/cms/adp/35/files/1675852160-22Jburlhnn.pdf
- Associação Portuguesa para a Promoção do Hidrogénio. n.d. Sobre o Hidrogénio. https://www.ap2h2.pt/sobre-h2.php
- Bacquart, T., Murugan, A., Carré, M., Gozlan, B., Auprêtre, F., Haloua, F., Aarhaug, T. A. 2018. Probability of occurrence of ISO 14687-2 contaminants in hydrogen: Principles and examples from steam methane reforming and electrolysis (water and chlor-alkali) production processes model. International Journal of Hydrogen Energy, 43, no. 26:11872-11883. https://doi.org/10.1016/j.ijhydene.2018.03.084.
- BASF. 2021. Adsorbents Solutions for Compressed Air Drying. https://catalysts.basf.com/files/literature-library/BASF_CAT-002485_Sorbead_Air_Broschuere_Update_03.pdf
- Bexiga, R. 2021. Development of a Hydrogen Drying Unit by Adsorption Processes. Master Thesis, Faculty of Engineering of the University of Porto.
- Corporate Finance Institute. 2022. Levelized Cost of Energy (LCOE). https://corporatefinanceinstitute.com/resources/valuation/levelized-cost-of-energy-lcoe/
- Dawood, F., Anda, M., Shafiullah, G.M. 2020. Hydrogen production for energy: An overview. International Journal of Hydrogen Energy, 45, no. 7: 3847-3869. https://doi.org/10.1016/j.ijhydene.2019.12.059.
- Delapedra-Silva, V., Ferreira, P., Cunha, J., Kimura, H. 2022. Methods for Financial Assessment of Renewable Energy Projects: A Review. *Processes*, 10, no. 2: 184. https://doi.org/10.3390/pr10020184
- Dincer, I., Acar, C. 2015. Review and evaluation of hydrogen production methods for better sustainability. International Journal of Hydrogen Energy, 40, no. 34: 11094-11111. https://doi.org/10.1016/j.ijhydene.2014.12.035.
- Du, Z., Liu, C., Zhai, J., Guo, X., Xiong, Y., Su, W., He, G. 2021. A Review of Hydrogen Purification Technologies for Fuel Cell Vehicles. Catalysts, 11, no. 3: 393. https://doi.org/10.3390/catal11030393
- Ferreira, D., Magalhães, R., Taveira, P., Mendes, A. 2011. Effective Adsorption Equilibrium Isotherms and Breakthroughs of Water Vapor and Carbon Dioxide on Different Adsorbents. Industrial & Engineering Chemistry Research, 50, no. 17: 10201-10210. https://doi.org/10.1021/ie2005302

- Fuel Cells and Hydrogen Observatory. 2022. Levelised Cost of Hydrogen. https://www.fchobservatory.eu/observatory/technology-and-market/levelised-cost-of-hydrogen-grid-connected-electrolysis
- Golmakani, A., Fatemi, S., Tamnanloo, J. 2017. Investigating PSA, VSA, and TSA methods in SMR unit of refineries for hydrogen production with fuel cell specification. Separation and Purification Technology. 176: 73-91. https://doi.org/10.1016/j.seppur.2016.11.030
- Hydrogen Council. 2022. Hydrogen Insights. https://hydrogencouncil.com/en/hydrogen-insights-2022/
- IDEALHY - Integrated Design for Efficient Advanced Liquefaction of Hydrogen. n.d. Liquid Hydrogen Outline. https://www.idealhy.eu/index.php?page=lh2_outline
- International Energy Agency. 2020. Projected Costs of Generating Electricity 2020. https://www.iea.org/reports/projected-costs-of-generating-electricity-2020
- International Energy Agency. 2021. Global Hydrogen Review 2021. https://www.iea.org/reports/global-hydrogen-review-2021/executive-summary
- International Energy Agency. 2022. Global average levelised cost of hydrogen production by energy source and technology, 2019 and 2050. https://www.iea.org/data-and-statistics/charts/global-average-levelised-cost-of-hydrogen-production-by-energy-source-and-technology-2019-and-2050
- International Energy Agency. 2022. Global Hydrogen Review 2022. https://iea.blob.core.windows.net/assets/c5bc75b1-9e4d-460d-9056-6e8e626a11c4/GlobalHydrogenReview2022.pdf
- International Organization for Standardization. 2019. Hydrogen fuel quality — Product specification. https://www.iso.org/obp/ui/#iso:std:iso:14687:ed-1:v1:en
- International Renewable Energy Agency. 2022. Geopolitics of the Energy Transformation: The Hydrogen Factor. https://www.irena.org/-/media/Files/IRENA/Agency/Publication/2022/Jan/IRENA_Geopolitics_Hydrogen_2022.pdf
- Jang, D., Kim, J., Kim, D., Han, W., Kang, S. 2022. Techno-economic analysis and Monte Carlo simulation of green hydrogen production technology through various water electrolysis technologies. Energy Conversion and Management, 258, 115499. https://doi.org/10.1016/j.enconman.2022.115499.
- Kohl, A. L., Nielsen, R. B. 1997. Gas Dehydration and Purification by Adsorption. In Gas Purification. Gulf Publishing Company.
- Leiblein, J., Bär, K., Graf, F., Hotz, C., Mörs, F. 2021. Techno-Economic Analysis of Green Hydrogen Production from Solar Energy in Mena and Transport to Central Europe. International Solar Energy Society. DOI:10.18086/swc.2021.01.01

- Ligen, Y., Vrubel, H., Girault, H. 2020. Energy efficient hydrogen drying and purification for fuel cell vehicles. International Journal of Hydrogen Energy, 45. no. 18: 10639-10647. https://doi.org/10.1016/j.ijhydene.2020.02.035.
- Megía, P. J., Vizcaíno, A. J., Calles, J. A., Carrero, A. 2021. Hydrogen Production Technologies: From Fossil Fuels toward Renewable Sources. A Mini Review. Energy Fuels, 35, no. 20: 16403-16415. https://doi.org/10.1021/acs.energyfuels.1c02501
- Nordio, M., Wassie, S. A., Annaland, M. V. S., Tanaka, D. A. P., Sole, J. L. V., Gallucci, F. 2021. Techno-economic evaluation on a hybrid technology for low hydrogen concentration separation and purification from natural gas grid. International Journal of Hydrogen Energy, 46, no. 45: 23417-23435. https://doi.org/10.1016/j.ijhydene.2020.05.009
- OIM Chemical. 2022. Activated Alumina vs Silica Gel. https://www.oimchem.com/technical-article/activated-alumina-vs-silica-gel.html
- Peters, M. S., Timmerhaus, K. D., West, R. E. 2003. Plant Design and Economics for Chemical Engineers. McGraw-Hill.
- Pinto, A. 2022. Optimization of a hydrogen drying unit by adsorption processes. Master Thesis, Faculty of Engineering of the University of Porto.
- Pourhakkak, P., Taghizadeh, A., Taghizadeh, M., Ghaedi, M., Haghdoust, S. 2021. Fundamentals of adsorption technology. In Adsorption: Fundamental Processes and Applications, edited by Mehrorang Ghaedi, 33: 1-70.
- Rousseau, R. W. 1987. Handbook of Separation Process Technology. Wiley-Interscience.
- Ruthven, D. M. 1984. Principles of Adsorption and Adsorption Processes. Wiley-Interscience
- Ruthven, D. M., Farooq, S., Knaebel, K. S. 1994. Pressure Swing Adsorption. VCH.
- Seader, J. D., Henley, E. J., Roper, D. K. 2011. Separation Process Principles. John Wiley & Sons, Inc.
- Seider, W. D., Seader, J. D., Lewin, D. R. 2003. Product and Process Design Principles. John Wiley & Sons, Inc.
- Skarstrom, C.W. 1963. Process for the recovery of hydrogen from hydrocarbon gas streams. Esso Research and Engineering Co: USA.
- Towering Skills. 2023. Cost Indices. https://www.toweringskills.com/financial-analysis/cost-indices/
- U.S. Department of Energy. n.d. Hydrogen Delivery. https://www.energy.gov/eere/fuelcells/hydrogen-delivery
- U.S. Department of Energy. n.d. Hydrogen Storage. https://www.energy.gov/eere/fuelcells/hydrogen-storage

- University of Calgary. n.d. Energy density. https://energyeducation.ca/encyclopedia/Energy_density
- Veras, T. S., Mozer, T. S., Santos, D. C. R. M., César, A. S. 2017. International Journal of Hydrogen Energy, 42, no. 4: 2018-2033. https://doi.org/10.1016/j.ijhydene.2016.08.219.
- Vermaak, L., Neomagus, H. W .J. P., Bessarabov, D.G. 2021. Recent Advances in Membrane-Based Electrochemical Hydrogen Separation: A Review. *Membranes*, 11, no. 2:127. https://doi.org/10.3390/membranes11020127
- Zhao, S. 2021. Thermochemical processes for biohydrogen production. In Waste to Renewable Biohydrogen, edited by Zhang, Q., He, C., Ren, J., Goodsite, M., Academic Press: 139-17. https://doi.org/10.1016/B978-0-12-821659-0.00011-3

Annex A - Hydrogen Fuel Quality Standards

The emerging technology of PEM fuel cells is accompanied with constraints for hydrogen quality.

ISO 14687:2019 specifies the minimum quality characteristics of hydrogen to be utilized as fuel in vehicular and stationary applications.

Hydrogen fuel is classified according to types and grade designations, as listed in Table A.1.

Table A.1 - Hydrogen and hydrogen-based fuel classification by application.

Type	Grade	Category	Applications
I (Gas)	A	-	Gaseous hydrogen; internal combustion engines for transportation; residential/commercial combustion appliances (e.g. boilers, cookers and similar applications)
	B	-	Gaseous hydrogen; industrial fuel for power generation and heat generation except PEM fuel cell applications
	C	-	Gaseous hydrogen; aircraft and space-vehicle ground support systems except PEM fuel cell applications
	D	-	Gaseous hydrogen; PEM fuel cells for road vehicles
	E	PEM fuel cells for stationary appliances	
		1	Hydrogen-based fuel; high efficiency/low power applications
		2	Hydrogen-based fuel; high power applications
		3	Gaseous hydrogen; high power/high efficiency applications
II (Liquid)	C	-	Gaseous hydrogen; high power/high efficiency applications
	D	-	PEM fuel cells for road vehicles
III (Slush)	-	-	Aircraft and space-vehicle on-board propulsion

The quality of hydrogen for grade D hydrogen must meet the requirements of Table A.2.

Table A.2 - Fuel quality specification for PEM fuel cell road vehicle application.

Constituents	Value
Hydrogen Fuel Index (minimum, %)	99.97
Total Gases (maximum, ppmv)	300
Water (maximum, ppmv)	5
Total Hydrocarbons (maximum, ppmv)	2
Methane (CH4)	100
Oxygen (maximum, ppmv)	5
Helium (maximum, ppmv)	300
Nitrogen and Argon (maximum, ppmv)	300
Carbon Dioxide (maximum, ppmv)	2
Carbon Monoxide (maximum, ppmv)	0.2
Total Sulfur Compounds (maximum, ppmv)	0.004
Formaldehyde (maximum, ppmv)	0.2
Formic Acid (maximum, ppmv)	0.2
Ammonia (maximum, ppmv)	0.1
Total Halogenated Compounds (maximum, ppmv)	0.05
Particulate Size (maximum, μm)	10

Appendix A: Equipment costs

A.1 Compressors

Purchase cost of compressors, C_P, was determined through Equation (B.1), where F_D and F_M are respectively the drive and material factors, with corresponding values of 1.25 for gas and 2.5 for stainless steel. The base purchase cost, C_B, which is given for a cost index of 394, is calculated by Equation (B.2), where P_C corresponds to the consumption in horsepower.

$$C_P = F_P \cdot F_M \cdot C_B \tag{A.1}$$

$$C_B = \exp(7.6084 + 0.80(\ln(P_C)) \tag{A.2}$$

A.2 Heat Exchangers

Heat exchangers purchase cost, C_P, was given by Equation B.3, where F_L is the length factor.

$$C_P = F_P \cdot F_M \cdot F_L \cdot C_B \tag{A.3}$$

The pressure factor, F_P, is obtained from equation B.4, where P represents pressure in psig.

$$F_P = 0.9803 + 0.018\left(\frac{P}{100}\right) + 0.0017\left(\frac{P}{100}\right)^2 \tag{A.4}$$

The material factor, F_M, is calculated through Equation B.5, where a and b depend on the construction material, taking the values of 1.75 and 0.13 and A is the outside tube area in ft^2.

$$F_M = a + \left(\frac{A}{100}\right)^b \tag{A.5}$$

The base cost, C_B, is given by Equation B.6, where A is the area in ft^2.

$$C_B = \exp(7.1248 + 0.16(\ln(A)) \tag{A.6}$$

A.3 Columns and storage tanks

Columns and tanks costs were determined based on the volume and mass of the stainless steel used in the equipment, which price is around 40 €·kg^{-1}, according to the company information.

A.4 Gas-liquid separators

The cost of gas-liquid separators was estimated making use of the power relationship known as the six-tenths factor rule, presented in Equation B.7, where X is the relation between the capacity of the existing equipment *b* and the desired equipment *a*.

$$C_a = C_b \cdot X^{0.6} \tag{A.7}$$

Appendix B: Walls thickness

In order to calculate the energy (q) required to heat the columns and, therefore, regenerate them, Equation B.1 was used.

$$q = m \cdot C_p \cdot \Delta T \tag{B.1}$$

The specific heat, $C_{p,}$ of the wall is shown in Table 3.1 and the change in temperature, ΔT, refers to the initial and regeneration temperatures in the columns. To determine the mass, m, of the columns, the thickness of the walls must be considered. It changes with diameter and pressure, and in this case, the same diameter was considered for the same flow rate and is also displayed in Table 3.1. The values for the wall thicknes are reported in Table B.1.

Table B.1 – Wall thickness for the different pressures and flow rates.

Feed flow rate	Units	20 bar	30 bar	40 bar
5 $Nm^3 \cdot h^{-1}$	mm	3	3	4
60 $Nm^3 \cdot h^{-1}$	mm	6	6	7
200 $Nm^3 \cdot h^{-1}$	mm	8	8	10
20000 $Nm^3 \cdot h^{-1}$	mm	20	28	35